

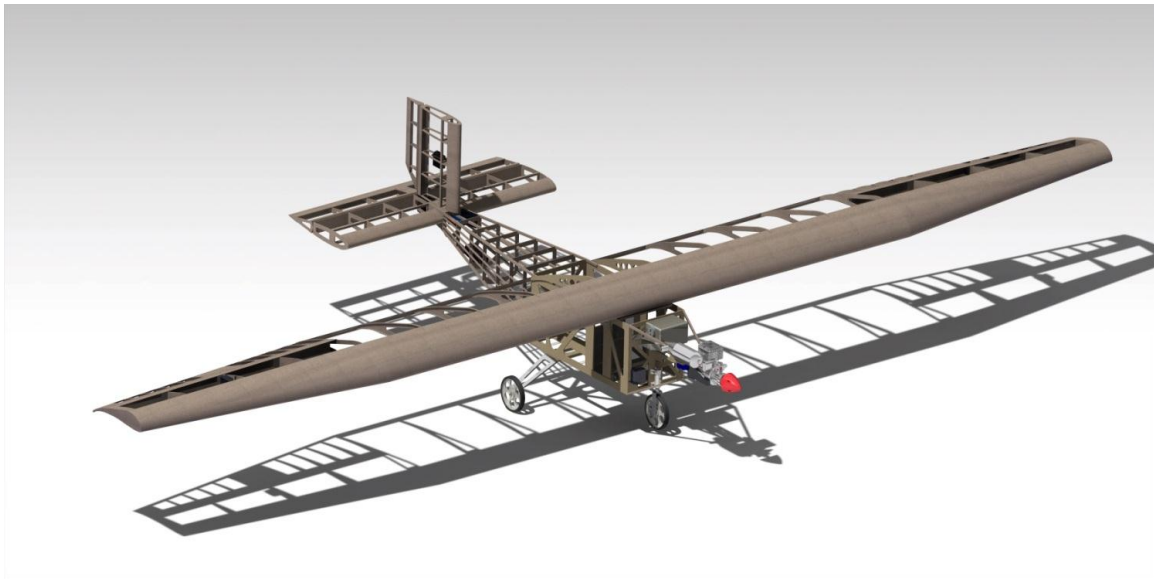
FIPSE: SAE Aero Design

Team 10 – Senior Design Final Report – April 2012

By

Dimitrios Arnaoutis¹, Alessandro Cuomo¹, Eduardo Krupa², Gustavo Krupa², Jordan Taligoski¹, David Williams¹

¹Department of Mechanical Engineering ²Departamento de Engenharia Mecânica



Project Sponsor

SAE International

FIPSE: Sustainable Energy and Aeronautical Engineering Program



Department of Mechanical Engineering

FAMU-FSU College of Engineering

2525 Pottsdamer St, Tallahassee, FL 32310

Contents

LIST OF SYMBOLS AND ACRONYMS	4
LIST OF FIGURES	5
LIST OF TABLES	7
1. ABSTRACT.....	8
2. INTRODUCTION.....	10
2.3 PROBLEM DESCRIPTION	11
2.3.1 Goal Statement.....	11
2.3.2 List of Objectives.....	11
2.3.3 Testing Environment	11
2.4 FUNCTIONAL DIAGRAM	14
2.5 QUALITY FUNCTION DEPLOYMENT.....	15
2.6 PROJECT PLAN	16
2.6.1 First Semester	16
2.6.2 Second Semester.....	17
3. CONCEPT GENERATION.....	18
3.1 CONCEPT 1: CONVENTIONAL DESIGN	18
3.2 CONCEPT 2: “FLYING WING” DESIGN	19
3.3 CONCEPT 3: MINIMALIST DESIGN	20
3.4 CONCEPT 4: CANARD WING DESIGN.....	21
3.5 CONCEPT 5: BI-PLANE DESIGN	22
3.6 CONCEPT SELECTION.....	23
4. FINAL CONCEPT – THE FLYING SPEAR.....	25
5. ENGINEERING ECONOMICS.....	27
6. RESULTS AND DISCUSSION	29
6.1 AERODYNAMICS	29
6.1.1 Profile Selection.....	29
6.1.2 Wing	30
6.1.3 Drag Polar.....	31
6.1.4 Flutter Analysis.....	31
6.1.5 Drag Analysis.....	32

7. STABILITY AND CONTROL.....	33
7.1 STATIC STABILITY.....	33
7.1.1 Longitudinal.....	33
7.1.2 Directional.....	34
7.1.3 Lateral.....	35
7.2 DYNAMIC STABILITY.....	35
7.2.1 Longitudinal and Lateral.....	35
7.2.2 Lateral-Directional.....	36
7.3 CONTROL.....	37
7.3.1 Elevator Analysis.....	37
7.3.2 Rudder Analysis.....	39
7.3.3 Aileron Design and Analysis.....	39
8. PERFORMANCE.....	40
8.1 POWER PLANT SELECTION.....	40
8.2 TAKE-OFF.....	41
8.3 FLIGHT PERFORMANCE.....	42
8.4 CLIMB AND GLIDE PERFORMANCE.....	42
8.5 TURNING PERFORMANCE.....	43
8.6 FLIGHT LEVEL.....	44
8.7 LANDING.....	44
8.8 MISSION TIME.....	44
9. LOADS AND STRUCTURE.....	45
9.1 STRUCTURAL DESIGN.....	45
9.2 FLIGHT ENVELOPE (V-N).....	45
9.3 MATERIALS PROPERTIES.....	45
9.4 WING LOAD DETERMINATION.....	46
8.5 SPAR SIZING.....	46
9.5 FRONT WHEEL.....	47
9.6 LANDING GEAR.....	47
9.7 LEVEL LANDING.....	48
9.8 LANDING ON TWO MAIN GEARS.....	48

9.10 WING	49
9.11 LANDING GEAR [MODEL]	49
9.12 WHEELS	49
9.13 AIRCRAFT EMPTY WEIGHT ESTIMATION	49
10. ELECTRICAL AND ELECTRONICS DESIGN	50
10.1 GENERAL CONSIDERATIONS.....	50
10.2 RADIO, RECEIVER AND SERVO SELECTION.....	50
10.3 ELECTRIC WIRE AND POWER DEMAND	50
10.4 BATTERY AND DEMAND CHARGE	51
10.5 VOLTWATCH AND VOLTAGE REGULATOR.....	51
10.6 ELECTRICAL DIAGRAM	52
11. ENVIRONMENT, HEALTH AND SAFETY	52
11.1 ENVIRONMENT	52
11.2 HEALTH	52
11.3 SAFETY	53
12. CONCLUSIONS	54
13. ACKNOWLEDGEMENTS	55
14. INTERNATIONAL EXPERIENCES	56
15. APPENDIX – SUPPORTING SOFTWARE DESCRIPTIONS.....	57
16. ENGINEERING DRAWINGS	59
17. REFERENCES.....	67
18. BIOGRAPHICAL SKETCH	69

List of Symbols and Acronyms

h – Height
 α – Angle of Attack
 δ_{Trim} – Elevator Deflection Angle
 δ_a – Aileron Deflection Angle
 Λ – Sweep Angle
 S – Surface Area
 CG – Center of gravity
 C_D – Aircraft Drag Coefficient
 C_d – Profile Drag Coefficient
 C_{D0} – Parasite Drag Coefficient
 C_L – Lateral Stability Coefficient
 C_h – Hinge Moment Coefficient
 C_m – Moment Coefficient
 C_n – Directional Moment Coefficient
 C_{m0} – Moment Profile Coefficient
 η_v – Dynamic Pressure
 C_L – Aircraft Lift Coefficient
 C_l – Profile Lift Coefficient
 C_V – Volume Coefficient
 c – Chord
 MAC – Mean Aerodynamic Chord
 Δ – Deflection
 ρ – Air density
 D_L – Dimensional angular stability derivative of the rolling moment
 N – Dimensional stability derivative
 Y – Dimensional Lateral Stability Derivative
 d – Distance

Index

a – Approach
 a_1 – Aileron
 ψ – Slip Angle
 β – Yaw angle
 w – Wing
 ac – Aerodynamic Center
 c – Cruise
 ds – Descend
 d – Dynamic
 dr – Dutch roll

s – Spiral
 EH – Horizontal stabilizer
 EV – Vertical stabilizer
 fus – Fuselage
 i – Induced
 A – Maneuver
 D – Dive
 ml – Spring
 p – Pitch
 np – Neutral Point

l_{CG} – CG distance – landing gear (x-direction)
 h_{CG} – CG distance – landing gear(y direction)
 X – Distance (x-axis)
 η – Efficiency
 b – Wingspan
 ζ – Damping Factor
 c_{at} – Friction Factor
 e – Oswald's Factor
 K – Pitch moment empirical factor
 D – Drag Force
 R – Reaction Force
 L – Lift Force
 ω – Frequency
 l – Width
 E – Modulus of Elasticity
 M – Moment
 I – Inertia Moment
 W – Weight
 P – Power
 q – Dynamic Pressure
 r – Radius
 k – Radius of Gyration
 A, AR – Aspect Ratio
 A_1 – Inertia moment Ratio
 η_{EH} – Relation between q_{EH}/q
 Re – Reynolds
 T – Thrust
 V – Speed
 μ – Air Viscosity
 Vol – Volume

B – Gust
 G – Gear Ratio
 rd – Wheel
 g – Ground
 td – Touchdown
 tr – Transition
 tp – Landing Gear
 v – Vertical
 r – Ya

List of Figures

I.	FIGURE 3.1: EXAMPLE OF A CONVENTIONAL DESIGN	18
II.	FIGURE 3.2: EXAMPLE OF FLYING WING DESIGN	19
III.	FIGURE 3.3.2: EXAMPLE OF MINIMALIST DESIGN	20
IV.	FIGURE 3.3.1: UFPR AIRCRAFT TAILBOOM WITH 2 CARBON FIBER TUBES	20
V.	FIGURE 3.4: EXAMPLE OF JET USING CANARD STYLE WING.....	21
VI.	FIGURE 3.5: BI-PLANE DESIGN SEEN AT THE BRAZIL AERODESIGN COMPETITION.....	22
VII.	FIGURE 4.1: 3D MODEL OF <i>FLYING SPEAR v.1</i>	25
VIII.	FIGURE 5.1: PIE CHART BREAKDOWN OF COSTS FOR THE PROJECT	28
IX.	FIGURE 6.1: AIRFOIL PROFILE	30
X.	FIGURE 6.2: AIRCRAFT DRAG POLAR.....	31
XI.	FIGURE 6.3: PERCENT OF DRAG CONTRIBUTIONS FROM EACH COMPONENT	33
XII.	FIGURE 7.2: UNIT IMPULSE LONGITUDINAL ELEVATOR RESPONSE	36
XIII.	FIGURE 7.3: ROOTS IN RELATION TO $Cn\beta$	36
XIV.	FIGURE 7.4: ELEVATOR DEFLECTION VS. CL AIRCRAFT.....	38
XV.	FIGURE 7.5.1: SPEED VS. ELEVATOR DEFLECTION.....	38
XVI.	FIGURE 7.5.2: FORCE ON ELEVATOR VS. SPEED	38
XVII.	FIGURE 7.6: FORCE ON RUDDER VS. SPEED	39
XVIII.	FIGURE 7.7: FORCE ON AILERON VS. SPEED (RUDDER AT 0°)	39
XIX.	FIGURE 7.8: FORCE ON AILERON VS. SPEED (RUDDER AT 20°).....	39
XX.	FIGURE 8.1: AVAILABLE THRUST VS. SPEED.....	40
XXI.	FIGURE 8.3: AIRCRAFT THRUSTS AND DRAGS	41
XXII.	FIGURE 8.2: AVAILABLE THRUST AND REQUIRED THRUST	41
XXIII.	FIGURE 8.4: PAYLOAD VS. TAKE-OFF DISTANCE VARYING ALTITUDE	42
XXIV.	FIGURE 8.5: CLIMB RATE	42
XXV.	FIGURE 8.6: DESCENT RATE	43
XXVI.	FIGURE 8.7: TOTAL MASS VS. TURNING ANGLE	43
XXVII.	FIGURE 8.8: TOTAL WEIGHT VS. MINIMUM TURNING RADIUS.....	43
XXVIII.	FIGURE 9.1: V-N DIAGRAM.....	45
XXIX.	FIGURE 9.3: BENDING MOMENT DIAGRAM	46
XXX.	FIGURE 9.2: SHEAR STRESS DIAGRAM	46
XXXI.	FIGURE 9.5: TORSION ANALYSIS	47
XXXII.	FIGURE 9.4: BENDING ANALYSIS	47
XXXIII.	FIGURE 9.6: LANDING GEAR I	48

XXXIV. FIGURE 9.7: LANDING GEAR II 48

XXXV. FIGURE 10.1: CURRENT IN FUNCTION OF TIME IN THE SERVOS CS-64 AND CS-12 51

XXXVI. FIGURE 10.3: ELECTRICAL DIAGRAM 52

List of Tables

I.	TABLE 1: DECISION MATRIX FOR CONCEPT DESIGN	24
II.	TABLE 4.1: SUMMARY OF COMPONENT’S CHARACTERISTICS FOR THE <i>FLYING SPEAR V.1</i>	26
III.	TABLE 4.2: OVERALL BUDGET SUMMARY TABLE FOR THE <i>FLYING SPEAR</i>	27
IV.	TABLE 6.1: PROFILE SELECTION	29
V.	TABLE 6.2: COMPARISON OF VARIOUS WING, PLANFORM AND TAIL GEOMETRIES	30
VI.	TABLE 7.1: VALUES FOR THE LONGITUDINAL STABILITY	34
VII.	TABLE 7.2: STATIC DIRECTIONAL STABILITY TABLE	34
VIII.	TABLE 7.3: ROOTS OBTAINED	36
IX.	TABLE 7.4: HINGE MOMENT COEFFICIENTS	37
X.	TABLE 8.1: ENGINE CHARACTERISTICS	40
XI.	TABLE 8.2: POWER PLANT STATIC TEST	40
XII.	TABLE 8.3: TAKE-OFF DATA SUMMARY	42
XIII.	TABLE 8.4: CHARACTERISTIC SPEED FOR 0 [M] AND 1100 [M]	42
XIV.	TABLE 8.5: RATE OF CLIMB	42
XV.	TABLE 8.6: DESCENT RATE	43
XVI.	TABLE 8.8: IDEAL FRICTION COEFFICIENTS	44
XVII.	TABLE 8.7: LANDING CHARACTERISTICS	44
XVIII.	TABLE 8.9: FLIGHT TIME	44
XIX.	TABLE 8.10: AVERAGE FUEL CONSUMPTION	44
XX.	TABLE 9.1: V-N DIAGRAM PARAMETERS	45
XXI.	TABLE 9.2: PERCENTAGE OF APPLIED LOAD IN EACH SECTOR IN RELATION TO THE TOTAL LOAD APPLIED ON THE WING SEMISPAN	49
XXII.	TABLE 9.3: BENDING RECORDED AFTER THE LOAD IN EACH WING SEMISPAN	49
XXIII.	TABLE 10.1: CHARACTERISTICS OF SERVOS UTILIZED	50
XXIV.	TABLE 10.2: BATTERY SPECIFICATIONS	51
XXV.	TABLE 10.3: CURRENT DEMAND	51
XXVI.	TABLE 10.4: VOLTAGE REGULATOR SPECIFICATIONS	51

1. Abstract

The purpose of our project is to compete in SAE Aero design East competition in the regular class; to be held in Mariette, Georgia April 27-29th. The purpose of the competition is to design, build and fly a lightweight remote controlled aircraft which can hold a significant amount of payload in comparison to its empty weight. The team consists of a variety of backgrounds; with the collaboration between students from Brazil and the United States.

Our needs assessments are outlined in the 2011-2012 regulations defined by SAE International that all teams participating in the competition must follow. Principle regulations for our aircraft in competition include: limitation of motor, constraints in the materials used, limitation in dimensions and gross weight of the aircraft, and a takeoff and landing requirements.

Knowing the competition requirements we were able to do basic sizing and develop a conceptual design and only after further analysis finalize a design prototype. The conceptual mockup carried out during the fall semester while spring semester was dedicated to the construction of our prototype design.

The entire aircraft was designed using the software CATIA, following various literatures to design, size and optimize various components of our aircraft. Primary design began with the aerodynamics of the plane and calculating lift and drag of various airfoils. The selected wing profile was a custom designed profile named the Uirá 1540 for both the root and the tip due to its low drag coefficient for the range of attack angles and high lift coefficient for the same conditions. Drag analysis was done on the basic design on all objects inducing drag (fuselage, landing gear, etc...) and the design was optimized. Stability and control of our design was analyzed using various literatures as well and with the software's AVL and a MATLAB code called Tornado VLM; this data was used to size the servo motors that control the dynamics of our airplane in flight. An estimated aircraft performance was evaluated using these predictions.

With the help of various literatures on aircraft design and aerodynamics coupled by the use of various programs, we were able to progress from needs assessment and a few educated assumptions to a preliminary design worthy of full fledge construction. Unfortunately, due to the complexity of the build, intermittent setbacks with our supplier and multiple schedules to work around we were not able to perform a test flight in time of writing of this report. However, in the near future we will have perform a test flight and remaining funds will allow for a second aircraft

to be constructed and brought with us to competition to better our chances at achieving high placement.

2. INTRODUCTION

2.1 Our Project

The team “The Flying Spear” began the fall semester of 2011 as an international design collaboration between two universities: Universidade Federal de Itajubá [UNIFEI] and Florida State University [FSU]. The team consists of 4 FSU students two of whom traveled to UNIFEI in the fall to study and participate in the SAE Brazil competition and two UNIFEI students currently studying at FSU who have previously been involved with aero design teams to work together on an international design project whose objective is to design a lightweight, high payload capacity aircraft while observing the available power and aircraft’s length, width, and height requirements as designated by the 2012 Regular Class requirements for the SAE Aerodesign competition.

This report illustrates the preliminary design studies and the main aircraft characteristics. It consists of the calculations and decisions made throughout the conceptual, preliminary and detailed design processes. The first section describes the overall aerodynamic characteristics of the aircraft while the next section covers the stability and control analysis which is important in order to validate the static and dynamic stability of the aircraft as well as the forces acting on the control surface. The final section describes the structural analysis conducted.

2.2 Needs Assessment

The proposed project is to design and build a cargo UAV fulfilling the 2011-2012 regulations and mission requirements as provided and defined by the SAE Aero Design East committee. This design must be documented by means of a technical report and a project presentation given to a panel of judges composed of aeronautical engineers. According to Dr. Leland M. Nicolai (Lockheed Martin engineer), *“The student needs to understand that the analysis and performance of the R/C model is identical to a full scale airplane such as a Cessna 172. The only differences between the R/C model and the full scale airplane are the wing loading, Reynolds Number and the moments of inertia”*.

The objective is to design an aircraft that can lift as much weight as possible meanwhile observing the available power and aircraft’s length, width, and height requirements as governed by the SAE Aero Design East committee. An important aspect to the design will be determining the lifting capacity of the aircraft as this could have an impact on the placement of different competing teams due to the availability of “bonus” points for correct predictions. With regards to

competition guidelines, the project is to be structured around three phases: a technical report, a technical presentation and inspection, and the physical flight competition. In order to do well in the competition, we need to excel in all three phases.

2.3 Problem Description

2.3.1 Goal Statement

Upon completion of this project we will have constructed a lightweight, fixed-wing remote-controlled aircraft possessing heavy payload lifting capacity. The aircraft must be able to takeoff in less than 61 meters, climb up and make a right turn completing a 360° lap and finally land carrying its maximum payload within 122 meters of runway. The following are desired characteristics that we hope to achieve for the aircraft: high L/D ratio (thus maximizing the entire flight envelope), high structural efficiency factor (possibly around 6.2), good maneuverability, and a high aspect ratio. We wish to incorporate all of these factors while maintaining a lightweight wing construction that is not significantly susceptible to C.G shifting; thus allowing the aircraft to fly without payload and earn the respective bonus points. It is expected that the aircraft will also have the capability to fly in a high wing load configuration while withstanding wind gusts. This is a major concern of the team because previous competitions several designs failed due to unaccounted wind gusts.

2.3.2 List of Objectives

- Design and construct an aircraft which minimizing the empty weight
- Design and construct an aircraft which has high payload lifting capacity
- Design and construct an aircraft that is easy for our pilot to control
- Place within the top 10 of the 75 teams competing in the SAE Aerodesign East competition

2.3.3 Testing Environment

The component testing environment was the garage of one of our team member's where most of the individual component were constructed and tested despite the fabrication of the landing gear system which was performed at the College of Engineering. Our flight testing environment is an R/C airfield 1.4 miles outside of Tallahassee's downtown. The airfield is

maintained by the Seminole Radio Control Club (SRCC) which is AMA (The Academy of Model Aeronautics) chartered club #216.

2.3.4 List of Constraints

Takeoff and Landing: During a takeoff (defined as the point at which the main wheels leave the ground), the aircraft must lift from the ground within a take-off distance requirement (**61 m**). During a landing, the aircraft must remain on the runway between their landing limits (**122 m**) to be considered a successful landing. Touch-and-goes are not allowed, and a crash-landing invalidates the landing attempt.

Engine Requirements: Regular Class aircraft can still be powered by a single, unmodified O.S 61FX with E-4010 Muffler.

Aircraft Dimension Requirement: Fully configured for takeoff, the free standing aircraft shall have a maximum combined length, width, and height of **225 inches**.

Gross Weight Limit: Regular Class aircraft may not weigh more than fifty five (**55 lbs**) pounds with payload and fuel.

Material Restriction: The use of Fiber-Reinforced Plastic (FRP) is prohibited on all parts of the aircraft. The only exception is the use of a commercially available engine mount and propeller. Exploration of other materials and building methods are greatly encouraged

Gear boxes, Drives, and Shafts: Gearboxes, belt drive systems, and propeller shaft extensions are allowed as long as a one-to-one propeller to engine RPM is maintained. The prop(s) must rotate at engine RPM.

Competition Supplied Fuel: The fuel for Regular Class entries will be a common grade, ten percent (10%) nitro methane fuel supplied by the Organizer.

Fuel Tanks: Fuel tanks must be accessible to determine contents during inspections. Tanks may be pressurized by a stock fitting on the engine muffler only.

Gyroscopic Assist Prohibited: No gyroscopic assist of any kind is allowed in the Regular Class.

Payload Distribution: The payload cannot contribute to the structural integrity of the airframe, and must be secured to the airframe within the cargo bay so as to avoid shifting while in flight.

Radios: The use of 2.4 GHz radio is required for all aircraft competing.

In-Flight Battery Packs: Regular Class aircraft must use a battery pack with no less than one thousand (1000) mAh capacity.

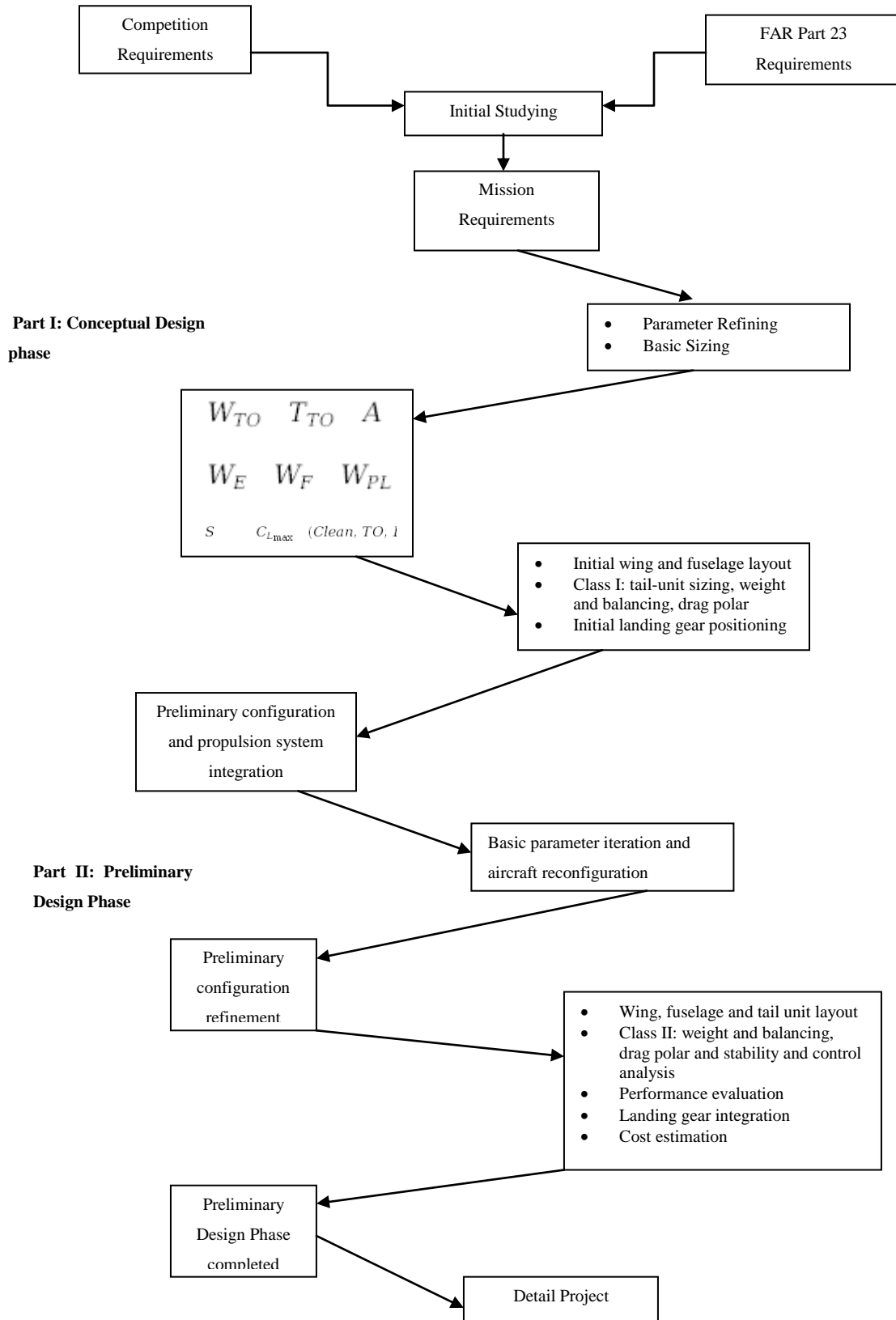
Spinners or Safety Nuts Required: All aircraft must utilize either a spinner or a rounded safety nut.

Metal Propellers Prohibited: Metal propellers are not allowed.

Control Surface Slop: Aircraft control surfaces must not feature excessive slop. Sloppy control surfaces lead to reduced controllability in mild cases, or control surface flutter in severe cases.

Servo Sizing: Analysis and/or testing must be described in the Design Report that demonstrates the servos are adequately sized to handle the expected aerodynamic loads during flight.

2.4 Functional Diagram



2.5 Quality Function Deployment

		Correlations									
		Positive +									
		Negative -									
		No Correlation									
		Relationships									
		Strong ●									
		Moderate ○									
		Weak ▽									
		Direction of Improvement									
		Maximize ▲									
		Target ◇									
		Minimize ▼									
Column #	1	2	3	4	5	6	7	8	9		
Direction of Improvement	▼	▼	▼	▼	▲	▼	◇	▲	▲		
Functional Requirements	Take off distance	Landing distance	Control surface slop	Empty weight	Lift capacity	Air drag	Maneuverability	Ease of control/flight	Structural strength		
Row #	1	2	3	4	5	6	7	8	9		
Customer Requirements (Explicit and Implicit)	Magnum XLS 61 Engine	255 inches combined dimension or less	55 lb combined weight or less	No FRP materials	No gearboxes on engine	10% nitromethane fuel	No gyroscopic assistance	Payload cannot contribute to structure	2.4 GHz radio	1000 mAh battery or greater	No metal propellers
	●			○	○		○				
			▽	●	●	●	▽			○	
	○	○	○		○						
	○	○	▽	●	●						●
	○			▽	○		●	▽			
	○				▽						
	▽	▽					○	●			
			▽	▽	▽	▽					●
			▽					▽			
	▽	▽		●	▽				▽		
			▽	▽							
Target	Less than 61 meters	Less than 122 m	No surface slop	Less than 3,85 kg	Greater than 14 kg		Turn 360 deg within field limitations	Easy to fly for the pilot			
Units	m	m	n/a	kg	kg	N	n/a	n/a	N		

2.6 Project Plan

The project was given a running time of one year. The first semester was used exclusively for design and analysis of the aircraft based on concept selection of individual components. Following the concept selection and analysis of first semester, the design was finalized and material ordering commenced. The second semester was devoted to construction of the aircraft, troubleshooting controls and completion of the design report submitted to SAE International as a part of our judging criterion.

2.6.1 First Semester

ID	Task Name	Duration	Start	Finish	Sep 4, '11							Sep 11, '11							Sep 18, '11							Sep 25, '11							Oct 2, '11							Oct 9, '11						
					S	M	T	W	T	F	S	S	M	T	W	T	F	S	S	M	T	W	T	F	S	S	M	T	W	T	F	S	S	M	T	W	T	F	S	S	M	T	W	T	F	S
1	Ice Breaker	7 days	Tue 9/6/11	Wed 9/14/11	[Bar]																																									
2	Code of Conduct	7 days	Tue 9/27/11	Wed 10/5/11															[Bar]																											
3	Rules Research	6 days	Tue 9/27/11	Tue 10/4/11															[Bar]																											
4	Needs Assessment/Project Scope	13 days	Tue 9/20/11	Thu 10/6/11															[Bar]																											
5	Register with SAE Aero East	55 days?	Tue 10/4/11	Mon 12/19/11																						[Bar]							[Bar]													
6	Product Specification/Project Plan	8 days	Tue 10/4/11	Thu 10/13/11																						[Bar]							[Bar]													
7	Design Research	40 days?	Mon 10/17/11	Fri 12/9/11																													[Bar]													
8	Wing Design Testing	5 days?	Mon 10/17/11	Sun 10/23/11																													[Bar]													
9	Fuselage Design Testing	5 days?	Mon 10/24/11	Sun 10/30/11																													[Bar]													
10	Controls Design Testing	5 days?	Mon 10/31/11	Sun 11/6/11																													[Bar]													
11	Materials Testing and Selection	5 days?	Mon 11/7/11	Sun 11/13/11																													[Bar]													
12	Order Parts	5 days?	Mon 12/5/11	Fri 12/9/11																													[Bar]													

ID	Task Name	Duration	Start	Finish	Oct 16, '11							Oct 23, '11							Oct 30, '11							Nov 6, '11							Nov 13, '11							Nov 20, '11						
					T	F	S	S	M	T	W	T	F	S	S	M	T	W	T	F	S	S	M	T	W	T	F	S	S	M	T	W	T	F	S	S	M	T	W	T	F	S	S	M	T	W
1	Ice Breaker	7 days	Tue 9/6/11	Wed 9/14/11																																										
2	Code of Conduct	7 days	Tue 9/27/11	Wed 10/5/11																																										
3	Rules Research	6 days	Tue 9/27/11	Tue 10/4/11																																										
4	Needs Assessment/Project Scope	13 days	Tue 9/20/11	Thu 10/6/11																																										
5	Register with SAE Aero East	55 days?	Tue 10/4/11	Mon 12/19/11	[Bar]							[Bar]							[Bar]							[Bar]							[Bar]													
6	Product Specification/Project Plan	8 days	Tue 10/4/11	Thu 10/13/11	[Bar]																																									
7	Design Research	40 days?	Mon 10/17/11	Fri 12/9/11								[Bar]							[Bar]							[Bar]							[Bar]													
8	Wing Design Testing	5 days?	Mon 10/17/11	Sun 10/23/11								[Bar]																																		
9	Fuselage Design Testing	5 days?	Mon 10/24/11	Sun 10/30/11								[Bar]																																		
10	Controls Design Testing	5 days?	Mon 10/31/11	Sun 11/6/11															[Bar]																											
11	Materials Testing and Selection	5 days?	Mon 11/7/11	Sun 11/13/11																						[Bar]																				
12	Order Parts	5 days?	Mon 12/5/11	Fri 12/9/11																													[Bar]													

3. Concept Generation

The general product specifications call for a lightweight, fixed-wing remote-controlled aircraft possessing heavy payload lifting capacity. The aircraft must be able to takeoff in less than 200 feet, ascend, turn completing a 360° lap and finally land in a designated landing zone of 400 feet while carrying its payload. Analyzing and converting the customer needs to product specifications, we have determined the following are desired characteristics for our aircraft: high L/D ratio, high structural efficiency factor, maneuverability, and a high aspect ratio. It is important to attempt to incorporate all of these factors while maintaining a lightweight wing construction as surely this is of utmost importance in our design.

3.1 Concept 1: Conventional Design

The conventional aircraft design layout is exactly what its name insists, conventional. This has been the chosen design for flight since the early 1900's. The design has stood the test of time for several key reasons. One reason is because of its durability. The central fuselage allows for a sturdy back bone for the aircraft to be based on. It also allows adequate room for cargo, pilots, and passengers without disturbing the overall air foil dramatically. Possibly it's most important trait is its stability. In most configurations the conventional style aircraft design is extremely stable allowing ease of flight and control. Within the conventional design there are several possible tail layouts that have their own flight characteristics.



Figure 3.1: Example of a conventional design with a tricycle main gear configuration

3.2 Concept 2: “Flying Wing” Design

A clean flying wing is theoretically the most aerodynamically efficient design configuration for a fixed wing aircraft. It also offers high structural efficiency for a given wing depth, leading to light weight and high fuel efficiency. Because it lacks conventional stabilizing surfaces or the associated control surfaces, in its purest form the flying wing suffers from the inherent disadvantages of being unstable and difficult to control. These compromises are difficult to reconcile, and efforts to do so can reduce or even negate the expected advantages of the flying wing design, such as reductions in weight and drag. This concept will require a special airfoil that makes the aircraft stable without a tail.



Figure 3.2: Flying wing example with turboprop engines mounted on the rear side of the aircraft

3.3 Concept 3: Minimalist Design

The minimalist design is intended to minimize the amount of material used to construct the aircraft while maintaining the integrity of a structurally sound, maneuverable airplane. Constructing an aircraft in this manner facilitates the possibility for creating a lightweight fuselage and airframe. These factors are important because minimizing the weight of the airframe gives one the ability to allocate more material to constructing a larger wing. A larger wing therefore provides more lift surface area for an optimized lift force. Many minimalist designs incorporate a “boom pole” style airframe rear which attaches to the aircraft’s aft. Not only does this reduce the total weight of the aircraft but it also minimizes the drag induced on the aircraft by the free flow air stream while in flight. It is plausible to use carbon composite tubing in combination with either a conventional tail or H-tail, in order to compensate for the possible loss in flight stability, to ensure the lightest weight while maintaining control of the aircraft. Some issues that may arise with this design option are the doubt in the aircraft’s ability to attain high wing load configurations in the presence of heavy wind gusts. Lacking uniformly distributed mass inhibits this capability thus the strength of the overall aircraft becomes of concern when weighed against variables that may not be in our control such as weather conditions.



Figure 3.3.1: UFPR aircraft implementing two carbon fiber tubes connecting the aft to the

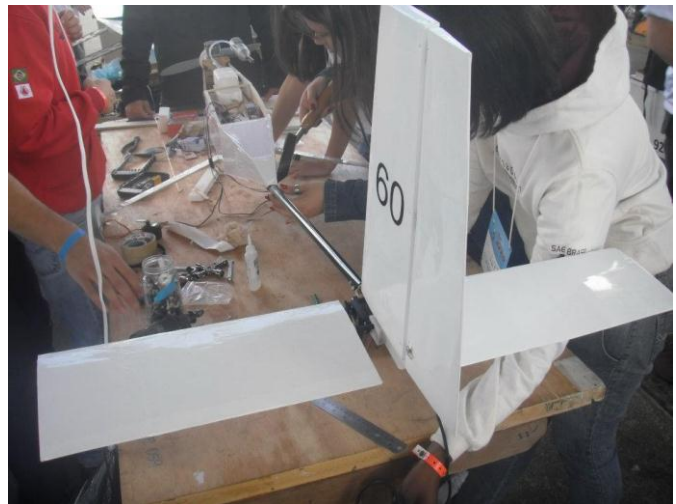


Figure 3.3.2: Lightweight, minimalist design featured at SAE Brazil Aerodesign competition

3.4 Concept 4: Canard Wing Design

Canard wing design is an application to aircraft that is not widely used. The basic idea behind the design is a two-wing application where the front wing is smaller than the back wing. On some designs, the front wing is almost as large as the rear wing. The main reason for this design is to increase lift on the aircraft. While this is accomplished by the unique wing layout, there can be negative effects, such as airflow disruption from the front wing to the back wing. When designing a canard wing system, it is very important to choose the appropriate length for the canard. There exists little room for error in this selection. The smallest change in length can drastically alter the flying performance of the aircraft. Throughout the years, many different types of planes have successfully adapted the canard wing design. From private use to military jets, canard wing design can be found in almost every type of application. Pictured below are some of the more successful designs.



Figure 3.4: Commercial jet using Canard style wing

3.5 Concept 5: Bi-Plane Design

A bi-plane is an aircraft with two fixed main wings. The bi-plane dominated aviation history for the first 30 years following the Wright brothers' Wright Flyer design. This wing structure influenced the Wright brothers from a civil engineer and his concepts in bridge building. Early airfoils were thin requiring external bracings, therefore the bi-plane is perfect as its arrangement and truss-like bridge structure provides for more structural efficiency than an externally braced monoplane.

Bi-planes are assumed to lift twice as much as a similar chord monoplane; however this is not the case. The wings actually interfere with the aerodynamics of one another, reducing lift and increasing drag. A simple alteration is seen in the case of tandem wing, when the bottom wing is placed at the front of the aircraft and top at the back, giving a advantage of 20% more lift than a single wing but also gives higher tip vortex drag than the equivalent monoplane. Bi-planes typically have a shorter wingspan however, giving greater maneuverability. Now with thicker stronger airfoils, the bi-plane is mainly used for recreation.

As for creating a RC bi-plane for competition, the advantages to the flight score look slim to none as drag is increased and lift is decreased to a standard monoplane, and any advantages to an alteration to the bi-plane (tandem) will be time consuming and difficult to perfect. The large size and structure of the biplane maybe costlier in terms of material costs and build time. Advantages will come in form of lightweight and strong wings wing structure and greater maneuverability.



Figure 3.5: Bi-Plane design seen at the Brazil Aerodesign competition

3.6 Concept Selection

The monoplane model was adopted because of its low drag compared to a biplane configuration. The high-wing configuration gives a better aerodynamic efficiency and a higher lateral stability. The wing planform has a trapezoidal format, which can reach an Oswald factor of 0.99 by proper positioning and taper ratio selection. This aircraft also has an engine with a tractor configuration. Below is a decision matrix summarizing the weights and respective scores of the significant factors affecting the performance of our aircraft.

Table 1: Decision matrix outlining the significant factors and the respective score for each concept design

		Standard Design		“Flying Wing” Design		Minimalist Design		Canard Wing Design		Bi-Plane Design	
Selection Criteria	Weight	Rating	Weighed Score	Rating	Weighed Score	Rating	Weighed Score	Rating	Weighed Score	Rating	Weighed Score
Potential Lift	20%	7	1.4	9	1.8	8	1.6	8	1.6	7	1.4
Potential Drag	10%	4	0.4	8	0.8	9	0.9	2	0.2	3	0.3
Durability	15%	9	1.35	5	0.75	3	0.45	7	1.05	7	1.05
Cost	10%	5	0.5	5	0.5	8	0.8	3	0.3	4	0.4
Ease of Manufacture	5%	5	0.25	6	0.3	8	0.4	4	0.2	4	0.2
Potential Flight Score	40%	8	3.2	6	2.4	7	2.8	7	2.8	7	2.8
	100%		7.1		6.55		6.95		6.15		6.15

4. Final Concept – *The Flying Spear*

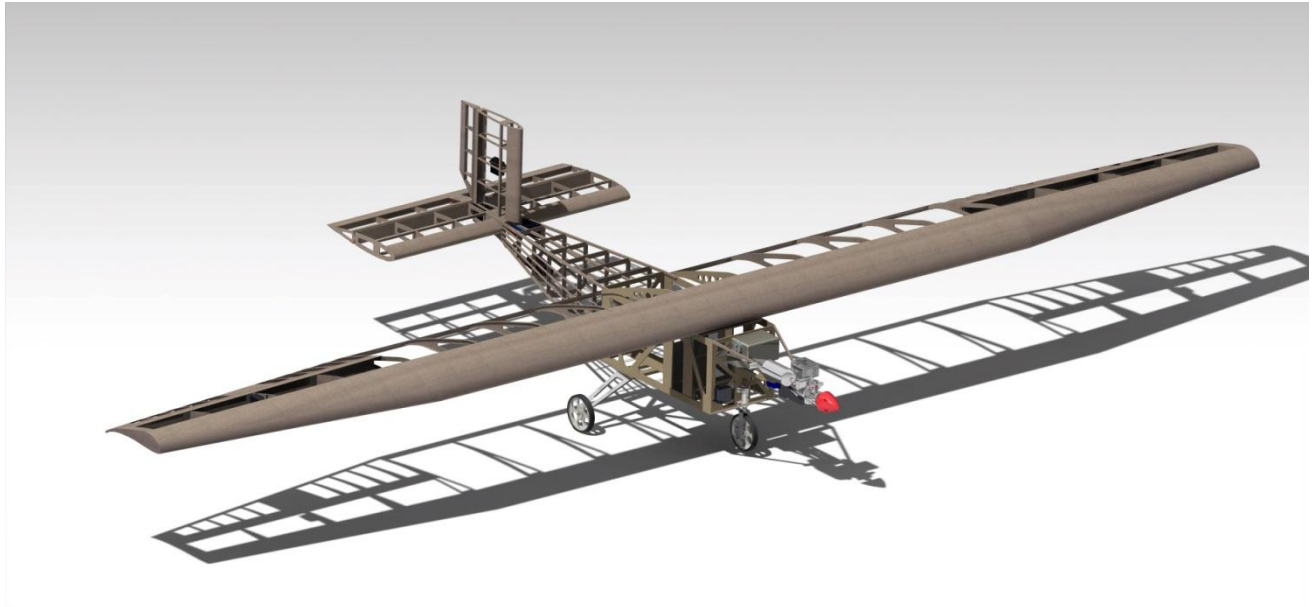


Figure 4.1: 3D detailed view of our prototype *Flying Spear v.1* done in CATIA software

The final concept design is that of a standard plane. There are five moving components of the design all controlled by servo motors. The right and left aileron controls the twist about the x-axis or the fuselage of the aircraft. On the tail of the aircraft there is an elevator which moves up and down, controlling the pitch of the aircraft. On the vertical stabilizer of the tail there is a rudder. The rudder will counter adverse yaw inflicted by the moving of the ailerons. The last servo mechanism is affixed to the front wheel, located under the engine, and is used to steer the aircraft while on the runway.

The landing gear configuration was chosen to be the tripod setup, which is the norm for small, standard shaped aircraft. The two rear wheels are attached to the fuselage by an aluminum support which was chosen for its characteristics of being both lightweight and strong.

Table 4.1: Summary of each component's characteristics for the *Flying Spear v.1*

Aircraft			
Conventional monoplane aircraft			
Aircraft Empty Weight	3.00 [kg]	Engine	Magnum XLS-61A
Wheel Diameter	7.50 [cm]	Engine angle of incidence	0°
Distance between axes and landing gear	28.5[cm]	Propeller	11x7 APC Nylon Sport
Distance between the wheels of the main landing gear	40.0[cm]	Servo-Mechanisms	HXT-900,CS-35MG,CS12MG,CS-64MG,CS-12MG
Wing			
High tapered wing			
Root profile	Uirá 1540	Tip Profile	Uirá 1540
Chord profile	32.0 [cm]	Tip Chord	20.0 [cm]
Wing height measured from the ground	36.8 [cm]	Wing Area	1.45 [m ²]
Wingspan	2.8 [m]	Aileron Area	696.25 [cm ²]
Aspect Ratio	10.5	Dihedral Angle	7°
Horizontal Stabilizer			
Full-deflection, type "H"			
Profile	NACA 0016	Area	1319.99[cm ²]
Chord	22.4 [cm]	Wingspan	60.0 [cm]
Vertical Stabilizer			
Duplo			
Profile	NACA 0016	Area	[cm ²]
Chord	20.0 [cm]	Wingspan	60.0 [cm]
Materials Utilized			
Balsa wood	Birch Plywood	Aluminum 6061	Nylon UHMW

5. Engineering Economics

Table 4.2: Overall budget summary table for the *Flying Spear*

Product	Price (\$)	Quantity	Total Cost (\$)
Registration/Travel	1100	1	1100
Plywood 3/32x1	22.59	8	180.72
Engine	173.17	1	173.17
Balsa 3/32x4x36	2.89	18	52.02
Ultracote	15.99	3	47.97
Balsa 1/8x4x36	3.19	9	28.71
11.1V battery	26.99	1	26.99
Plywood 12x24	22.49	1	22.49
10 oz glue	7.39	3	22.17
Fuel	16.99	1	16.99
48" Servo Wire	5.5	3	16.50
6V battery	15.99	1	15.99
Pushrods	7.25	2	14.50
5 min Epoxy	12.99	1	12.99
30 min Epoxy	12.99	1	12.99
36" Servo Wire	5.00	2	10.00
Power Switch	7.99	1	7.99
2 oz glue	6.99	1	6.99
6 oz Flextank	6.89	1	6.89
HXT-900 servo	6.49	1	6.49
CS-64 servo	26.99	1	26.99
CS-12MG servo	21.99	1	21.99
CS-35MG servo	24.99	3	74.97
Servo connect	2.89	2	5.78
Balsa 1/16x4x36	2.59	2	5.18
8 oz Fuel tank	5.15	1	5.15
Y-Harness	5.00	1	5.00
13x6 Propeller	4.90	1	4.90
Nylon Clevis	4.79	1	4.79
Bass cap strip	0.59	7	4.13
Aluminum Tube	2.99	1	2.99
11x6 Propeller	2.86	1	2.86
Wood Dowel	1.79	1	1.79
Threaded Rod 4x40	1.69	1	1.69
Threaded Rod 2-56	0.65	2	1.30
8 pc hex nut	0.85	1	0.85
		Total Expenditures	\$ 1952.92

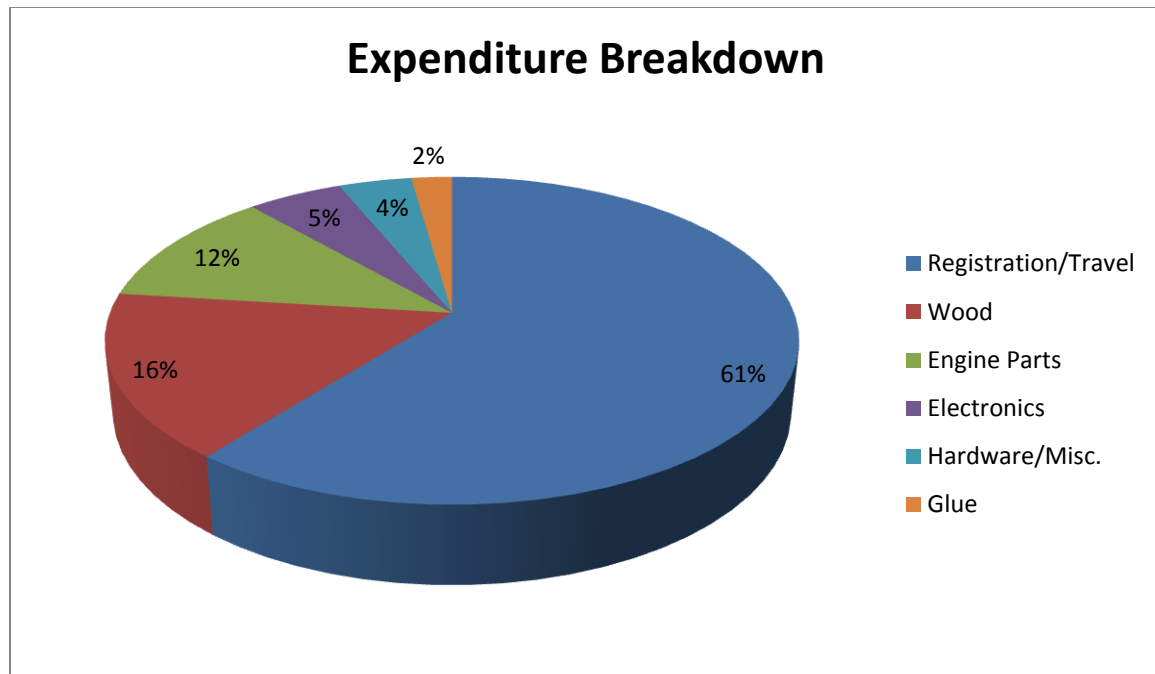


Figure 5.1: Pie chart illustrating the breakdown of costs for the project

As can be seen from our Bill of Materials, our registration and travel expenses for the SAE competition are the largest expenditure for our senior design project totaling to about \$600. This is almost two thirds of our total expenses however considering the finished product and the opportunity to compete in this competition we feel justified with the money we have spent. The breakdown of our expenditure is what we expected. Since our plane is fabricated almost entirely from balsa and plywood, it is understandably our second largest expenditure.

6. Results and Discussion

The design point set to the aircraft was at steady flight while carrying maximum payload and at cruise speed. The following constants were used according to the standard condition for temperature and the pressure: $\rho = 1.2250$ [kg/m³] and $\nu = 1789 \cdot 10^{-6}$ [N.s/m²]. The value adopted for the acceleration of gravity was 9.8067 [m/s²]. The inertia moments were obtained from detailed drawings by means of the software CATIA[®].

6.1 AERODYNAMICS

The aerodynamic detailed design started with the geometry created as a result of the preliminary project. This allowed the team to define the requirements for the aerodynamic design. The literature utilized was BARROS [3] and RAYMER [1]. The team attempted to maximize the factor L/D since it affects the aircraft during all flight phases.

6.1.1 Profile Selection

The initial requirements were to design a profile that has at least $C_{L_{max}} = 2.08$. This value was calculated assuming that the aircraft could achieve its take-off speed (as seen in the performance section) with our maximum payload of approximately 165 N.

The associated Reynolds regime is in the order of 215,000. According to WHITE [4], the transition for a turbulent boundary layer occurs with a local Reynolds number, Re_x , that can be taken as $2.8 \cdot 10^5$, where x is the leading edge distance. The value of $Re_{x_{crit}}^{1/2}$ depends on the turbulence intensity and is determined by the following semi-empirical relation where ζ is the turbulence intensity.

$$Re_{x_{crit}}^{1/2} = \frac{-1 + (1 + 13,25\zeta^2)^{1/2}}{0,00392\zeta^2} \quad (6.1)$$

Assuming a turbulence of $\zeta = 0.04$ and plotting this result against the speed, the laminar flow was extended along 3% of the chord.

Table 6.1 – Profile Selection

Profile	$t/c(\%)$	$f(\%)$	$C_{l_{max}}$	$C_{d_{min}}$	C_m	C_l/C_d	Stall Type
Uirá1590	13.51	8.66	2.33($\alpha = 15^\circ$)	0.0168736	-0.179	78.3	Smooth
Uirá1540	15.31	11.87	2.64($\alpha = 15^\circ$)	0.0198286	-0.202	66	Abrupt

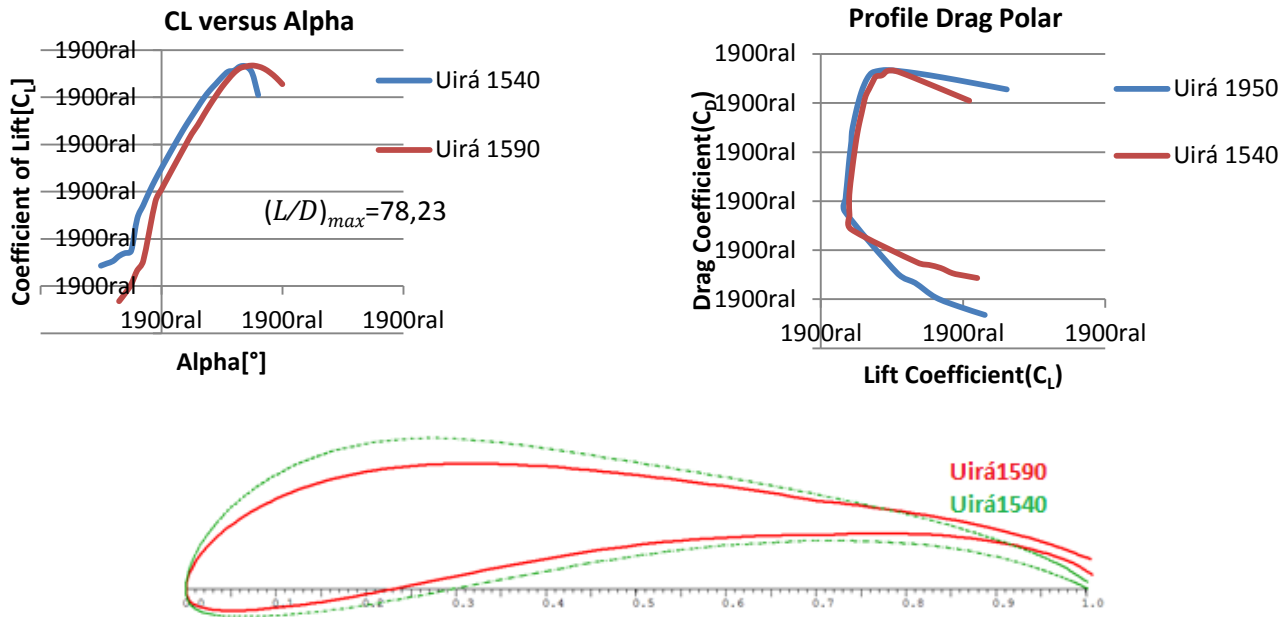


Figure 6.1: Airfoil Profile

6.1.2 Wing

The wing design methodology consisted of systematic variations of the following geometric factors: wing area, taper ratio and taper location. For each iteration the following parameters were studied: Oswald efficiency factor, $C_{L_{max}}$, $C_{D_{min}}$ and C_m . The main advantages and disadvantages considered are summarized in the **Error! Reference source not found.**

Table 6.2: Comparison of various wing positions, planform geometries and tail geometries

Characteristics		Advantages	Disadvantages
Wing Location	High Wing	Low interference drag, high lateral stability, shorter landing (less ground effect)	Take-off is longer because of the reduction of the ground effect
	Recto-trapezoidal	Combines the advantages of a rectangular and tapered wing in the sense that it exhibits reduced induced drag and has a smaller value for lateral inertia while being the most structurally sound option	The main disadvantage is the stall tendency in the aileron area
Empennage Type	Conventional Tail	Good response to the pitch command	Negative aerodynamic load in the horizontal empennage that may reduce the total lift
	T-tail	Only 2 points of aerodynamic interference, against 4 of the conventional tail	Building difficulties and deep stall risk

We selected the same profile from the wing root to the tip. The taper of the wing creates an area more susceptible to stall in the aileron; however, the stall must start at the beginning of the root to the tip and then over the ailerons in order to assure the lateral control of the aircraft even during the stall. For that we utilized the Armin Quast's orientation, found in BARROS [3], only after could we calculate a geometric twist of 2° .

6.1.3 Drag Polar

The drag polar was evaluated using a method proposed by BARROS [3] which takes into consideration the required elevator deflection to keep the aircraft in steady level flight. Also, it takes the length variations of the aerodynamic behavior of the components and their respective speed variations.

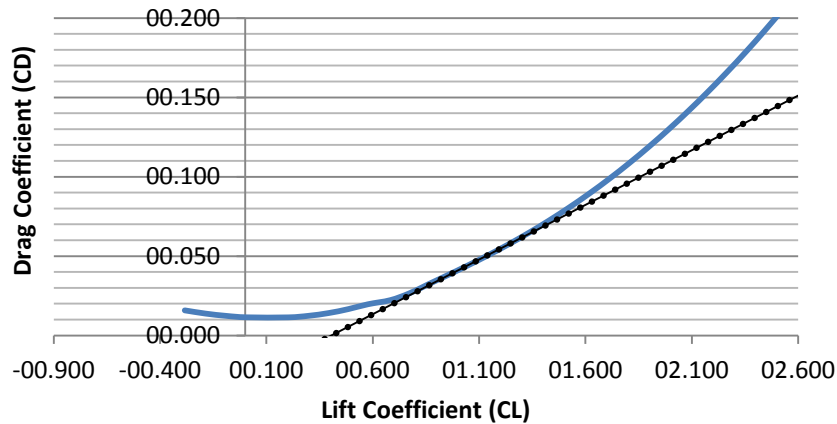


Figure 6.2: Aircraft Drag Polar

6.1.4 Flutter Analysis

Due to the wing having a very high aspect ratio, we had to perform a flutter analysis. To do so we utilized a criteria found in the paper *Simplified Flutter Prevention Criteria For Personal Type Aircraft* [5] which states that the torsion flexibility factor, F , given by the Equation 6.2, must be less than $200/V_d^2$.

$$F = \int Q_i C_i^2 ds \quad (6.2)$$

Where Q_i is the wing torsion on the station, i , caused by a unit torsional movement applied on the trailing edge of the station; C_i is the chord length of the wing in the station i [m]; ds is the increment of b . The strategy adopted was a less tapered wing with only one type of profile from

the root to the tip. According to the formulation exposed above, we obtain $F = 0.32404 < 0.413223$.

6.1.5 Drag Analysis

According to ANDERSON [7], the accuracy of the performance calculations depends on the quality of the aerodynamic data. The correct estimates of drag provide qualitative data used to make decisions during the aerodynamic design; therefore it is of the utmost importance for the correct evaluation of its actual capacities.

The team has consulted HOERNER [8] who expresses the aerodynamic forces in terms of dynamic pressure, utilizing the concept of drag area which is useful in cases where the reference area is not apparent. Therefore, this was used to estimate the contribution to drag from building and superficial imperfections. In this way it was possible to prevent the influence of each component to and redraw it when the drag was prohibitive, until we obtain a final configuration of most aerodynamic efficiency.

The method of the equivalent length was used in order to determine the C_{D0} of the aircraft lift surfaces. This presupposes that the friction drag contribution of each component is equivalent to a flat plate having the same wetted area and same characteristic length.

In order to estimate the wing C_{D0} , we assume that the fuselage influence over it is small, since the fuselage is located below the wing, presupposing a laminar flow over the fuselage. Therefore, the Equation 6.3 for a flat plate was used:

$$C_f = \frac{1,328}{\sqrt{Re_L}} \quad (6.3)$$

The contribution of the tail-unit to the drag was evaluated by considering the downwash produced by the wing, fuselage and the tail-boom interference over the empennage. We also assumed that the flow is turbulent. For flat plates, Equation 6.4 was utilized for the drag estimation and zero lift in a turbulent flow:

$$C_f = \frac{0,074}{Re_L^{0,2}} \quad (6.4)$$

In order to estimate the fuselage drag we have assumed that the flow is, since the beginning, turbulent due to the propeller slipstream. Therefore the Eckert Equation was utilized since it deals with a blunt body in a completely turbulent flow.

The proportionality coefficient deduced by Eckert are constants of values $A = 0.455$, $b = 2.58$, $c = 0.144$ and $d = 0.58$.

$$C_{f,turb} = \frac{A}{(\log Re)^{b(1+cM^2)^d}} \quad (6.5)$$

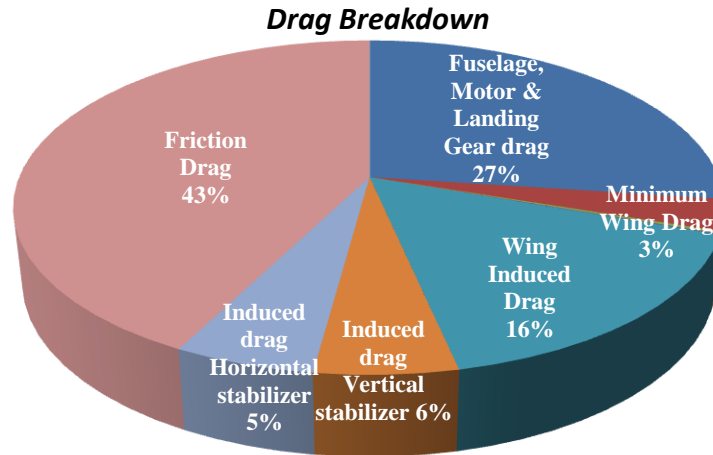


Figure 6.3: Percent of Drag Contributions from each component

7. STABILITY AND CONTROL

An aircraft is stable if after undergoing a disturbance it can return to its original position using the aircraft pitch, roll and yaw commands. The stability analysis is divided into static and dynamic analysis and is further divided into longitudinal, directional and lateral.

7.1 Static Stability

7.1.1 Longitudinal

For the static stability longitudinal analysis, RAYMER [1] affirms that the derivative of the pitch moment in relation to the angle of attack must be negative. The equation that applies to this case is given by:

$$Cm_{\alpha} = -C_{L\alpha}(X_{np} - X_{CG}) \quad (7.1)$$

Where X_{np} is the point in which $Cm_{\alpha} = 0$ and does not depend on the CG, RAYMER [1] says that the static margin must be positive and over 5%.

Using the *software Tornado*[®], the static margin was calculated. In the *software AVL*[®] we obtained X_{cg} and X_{np} , the subtraction of these two terms is equal to MS , therefore the obtained values confirm the values obtained. The data is presented in the Table 7.1.

Table 7.1 – Values for the Longitudinal Stability

X_{np}	X_{cg}	MS	$C_{L\alpha}$ [rad^{-1}]
0.1997	-0.0569	0.2567	5.5090

Replacing these values in the Equation 7.1 we get $Cm_\alpha = -1.4144$ [rad^{-1}]. According to CORKE [9], the Cm_α value must be negative and assume a value between -1.5 and -0.16. Since the Cm_α obtained is situated in this margin, we conclude that the aircraft is longitudinally stable.

7.1.2 Directional

The static stability directional analysis is given by, according to CORKE [9], the Cn_β coefficient.

$$Cn_\beta = (Cn_\beta)_{fus} + (Cn_\beta)_w + (Cn_\beta)_{EV} \quad (7.2)$$

The Table 7.2 presents the values obtained for the Cn_β calculation:

Table 7.2 – Static directional stability table

Fuselage		Wing		Stabilizer	
$l_{fus} = 0.5196$ [m]		$AR = 10.5$		$CV_{EV} = 0.035$	
$h_{fus} = 0.1746$ [m]		$\bar{c} = 0.290$ [m]		$\alpha_{EV}\eta_{EV} = 1.081$	
$Vol_{fus} = 0.01495$ [m ³]		$C_L = 2.080$ [rad^{-1}]		$(C_{L\alpha})_{EV} = 6.283$ [rad^{-1}]	
$S_w = 0.8600$ [m ²]		$X_{cg} = 0.03$ [m]		$(Cn_\beta)_{EV} = 0.2376$ [rad^{-1}]	
$(Cn_\beta)_{fus} = -0.007533$ [rad^{-1}]		$(Cn_\beta)_w = 0.03342$ [rad^{-1}]			

According to the same reference, the acceptable values for Cn_β must be contained between 0.08 and 0.28. Using the values showed in the Table 7.2 above we can obtain a value for $Cn_\beta = 0.2634$ [rad^{-1}]. Therefore following this method we conclude that the aircraft is directionally stable.

7.1.3 Lateral

For the lateral stability analysis, we use the $C\mathcal{L}_\beta$ coefficient (Equation 7.3) and this value must be less than zero. However since the terms of the equation are difficult to evaluate, CORKE [9] suggests an approximation, given by the Equation 7.4:

$$C\mathcal{L}_\beta = (C\mathcal{L}_\beta)_W + (C\mathcal{L}_\beta)_{EV} + (C\mathcal{L}_\beta)_{W-F} \quad (7.3)$$

$$C\mathcal{L}_\beta = -Cn_\beta \quad (7.4)$$

Following Corke, for the aircraft to be considered laterally stable the following inequality must hold: $-0.9 \leq \frac{C\mathcal{L}_\beta}{c_L} \leq -0.05$. As $C\mathcal{L}_\beta = -0.2634 [rad^{-1}]$ and $\frac{C\mathcal{L}_\beta}{c_L} = -0.1266 [rad^{-1}]$. We conclude the aircraft is laterally stable since the values found are less than zero.

7.2 Dynamic Stability

7.2.1 Longitudinal and Lateral

According to the norm JAR-VLA [12], every short period oscillation (not including the lateral-directional that occurs between the stall and the maximum speed) must be critically damped using the primary controls.

In order to evaluate the longitudinal dynamic analysis, the motion equations were written in a state-space format. This technique allows the motion variables to be written in transient form, which allows the team to evaluate the whole behavior of the aircraft during its flight envelope. This method makes use of the transfer function, where the input function represents small aircraft disturbances. This allows these equations to be solved by numerical methods. Using the software *MATLAB*[®], a complete evaluation could be made. The correspondent matrix equations are show below.

$$\overline{M}\dot{\mathbf{x}} = \overline{A}' + \mathbf{B}'\overline{U}(t) \quad (7.5)$$

$$M = \begin{bmatrix} m & -\dot{X}_w & 0 & 0 \\ 0 & (m - \dot{Z}_w) & 0 & 0 \\ 0 & -\dot{M}_w & I_y & 0 \\ 0 & 0 & 0 & 1 \end{bmatrix} \quad A' = \begin{bmatrix} \dot{X}_u & \dot{X}_w & (\dot{X}_q - m_{w_e}) & -mg\cos\theta_e \\ \dot{Z}_u & \dot{Z}_w & (\dot{Z}_q + m_{u_e}) & -mg\sin\theta_e \\ \dot{M}_u & \dot{M}_w & \dot{M}_q & 0 \\ 0 & 0 & 1 & 0 \end{bmatrix} \quad B' = \begin{bmatrix} \dot{X}_\eta & \dot{X}_\tau \\ \dot{Z}_\eta & \dot{Z}_\tau \\ \dot{M}_\eta & \dot{M}_\tau \\ 0 & 0 \end{bmatrix}$$

The aircraft response is calculated taking into account a 1° degree elevator deflection, and its correspondent transfer functions are determined adopting the hypothesis that the motion is

constrained to small disturbances. Observing the Figure 7.2 below, we conclude that this aircraft satisfies the requirements imposed by the norm.

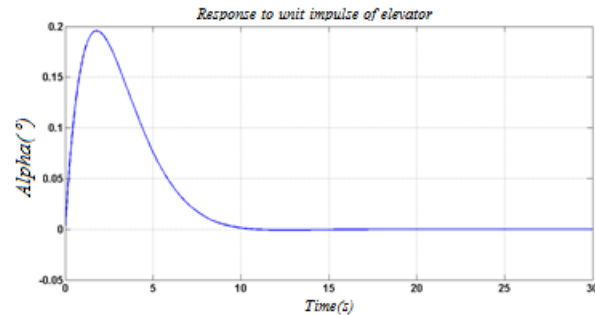


Figure 7.2: Unit impulse Longitudinal Elevator response

7.2.2 Lateral-Directional

NELSON [10] affirms that for a dynamic lateral-directional analysis, one must use the motion equations that take into account the lateral force, the roll moment and pitch moment. These can be rearranged in state-space format and then it will become possible to obtain the necessary derivatives. The stability calculations can be obtained by the relation given by the matrix below, where the values were calculated using the *software MATLAB*[®].

Following this method two real roots and two imaginary roots were found, that characterize the response to the spiral, dutch roll and roll modes. The values obtained for the roots are given below (Table 7.3), as the graph obtained (Figure 7.):

Table 7.3 – Roots obtained

λ (<i>spiral mode</i>)	$-0.0104 \cdot 10^2$
λ (<i>roll mode</i>)	$-2.9431 \cdot 10^2$
λ (<i>dutch roll mode</i>)	$-0.0221(\pm 0.0362i)$

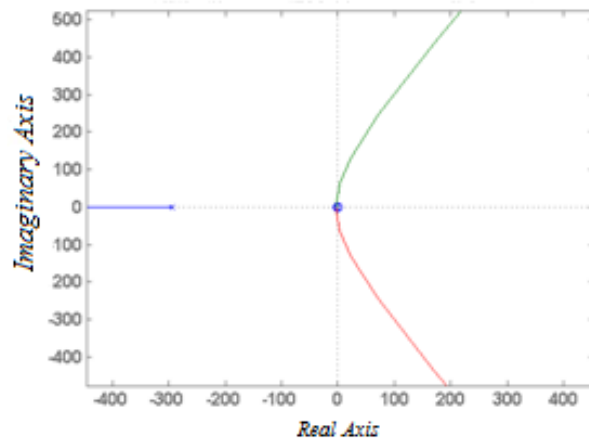


Figure 7.3 – Roots in relation to $C_{n\beta}$

Since the roots obtained are in the left semi-plane, by the classical control theory, we can assure that the aircraft is lateral-directionally stable.

7.3 Control

The concept of control is employed when one wants to change the flight conditions of the aircraft. This concept is important to the correct sizing of the aircraft servo-mechanisms. It also helps to size the control surfaces that better satisfy the necessities posed by the aircraft. For the control calculation it is necessary to obtain the hinge moment coefficients, obtained by the team using the *software AVL*[®] and recorded in Table 7.4.

Table 7.4 – Hinge Moment Coefficients

$Ch_{\delta EH} [rad^{-1}]$	$Ch_{\delta EV} [rad^{-1}]$	$Ch_{\delta aileron} [rad^{-1}]$
0.0786	-0.1941	-0.2214

7.3.1 Elevator Analysis

The following Equation 7.7 gives the speed required for a steady level flight.

$$V_{trim} = \sqrt{2 \cdot \frac{W}{\rho S C_{L_{trim}}}} \quad (7.6)$$

Considering a particular case in which we want to fly at a speed less than the cruise speed to compensate the dynamic pressure, we must increase the $C_{L_{trim}}$ on the same proportion. An increase in the $C_{L_{trim}}$ can be obtained in two ways: either increasing the deflection angle or shifting the aircraft CG location. Since the CG position is related to the cargo-bay geometry, we use the first option for the study of a longitudinal control. According to ANDERSON [2], the elevator deflection angle is given by the Equation 7.8. Its efficiency must be sufficient to produce a moment on the tail in relation to the C.G at the maximum take-off speed.

$$\delta_{trim} = \frac{C_{m0} + (C_{m\alpha}\alpha)}{v_{EH} C_{L\alpha EH}} \quad (7.7)$$

Where $C_{m0} = -0.1385 [rad^{-1}]$. In this way, varying the CG position we obtained the Figure 7.4.

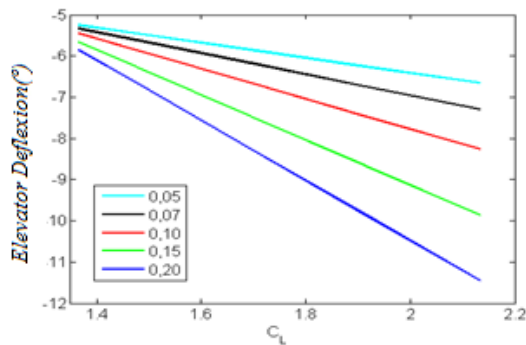


Figure 7.4: Elevator deflection vs. CL aircraft

Observing Figure 7.4, we conclude that the elevator deflection satisfies the values demanded during the flight for a variation between 5% to 20% of the static margin and they are capable of changing the profile camber generating in this way a hinge moment. TORENBEEK [11] indicates the Equation 7.9.

Integrating the Equation 7.9 and adopting a reference point ($\delta_{EH} = 0^\circ$ for $V = V_{trim}$), we could obtain the Figures 7.5.1 and 7.5.2.

$$\frac{\partial \delta_{EH}}{\partial V} = \frac{2C_L(X_{np} - X_{CG})S\bar{c}}{C_{LEH}V S_{EH} X_{EH}} \tag{7.8}$$

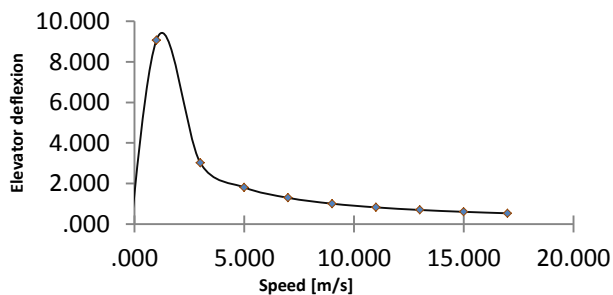


Figure 7.5.1: Speed vs. Elevator Deflection

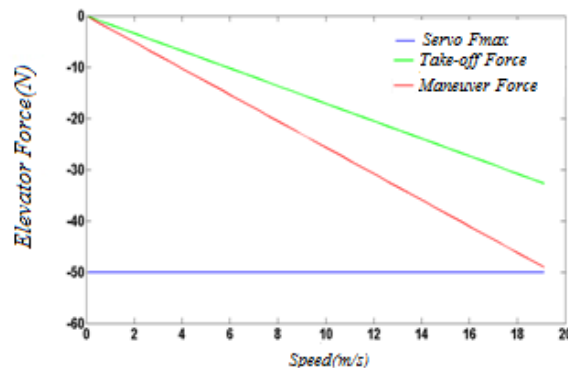


Figure 7.5.2: Force on elevator vs. Speed

We could analyze the force demanded by the elevator utilizing the moment equation as showed in the Figure 7.5.2, and size the servo for the elevator.

7.3.2 Rudder Analysis

RAYMER [1] characterizes an “efficient” rudder as one that has a chord length in relation to the vertical stabilizer between 25% and 50%. In the beginning the team has used the minimum value of 25%.

For the evaluation of the forces generated by the rudder, Equation 5.10 given by ROSKAN [6] was utilized:

$$\frac{\partial F_{EV}}{\partial \beta} = \frac{G_{EV} \eta_v q S_{EV} \bar{c}_{EV} Ch_{\delta EV} Cn_{\beta free}}{Cn_{\delta EV}} \quad (7.9)$$

Using the *software AVL*[®], we got $Cn_{\beta free} = 0.0995$ and $Cn_{\delta EV} = -0.0153$. Integrating the Equation 7.10 and knowing a point of this curve (the point where $F_{EV} = 0$ [N] for $Cn_{\delta EV} = 0^\circ$) we obtained the following Figure 7.6.

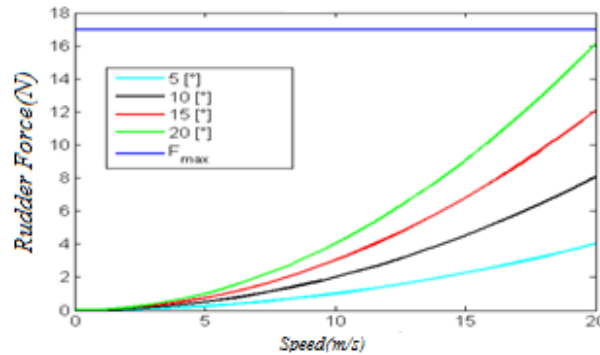


Figure 7.6: Force on rudder vs. Speed

By observing the Figure 7.6, we conclude that the force in the rudder is 17 [N].

7.3.3 Aileron Design and Analysis

Equation 7.11 given by ROSKAN [6] was utilized to evaluate the ailerons:

$$F_{al} = q S_{al} \bar{c}_{al} G_{al} (-2Ch_{\delta al} \delta_{al}) + G_{al} K_{EV-al} \delta_{EV} \quad (7.10)$$

Then, the following graphs were obtained:

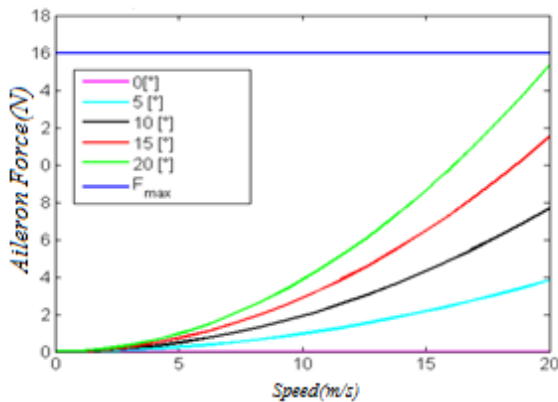


Figure 7.7: Force on aileron vs. Speed (Rudder at 0°)

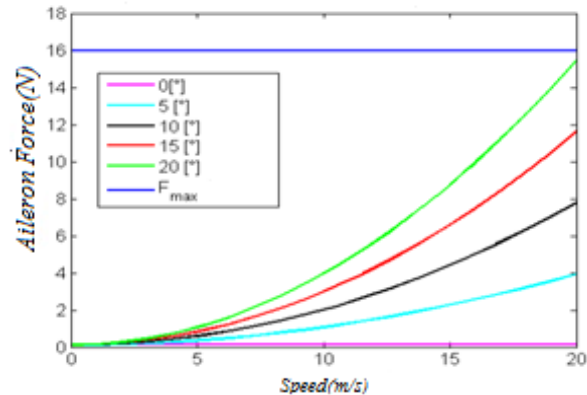


Figure 7.8: Force on aileron vs. Speed (rudder at 20°)

8. PERFORMANCE

8.1 Power Plant Selection

The selection of the power plant has great importance in the development of the aircraft design because the power plant has a crucial role in the mission that the aircraft was designed to accomplish.

The engines that were traditionally used by the competition are presented, with some of its characteristics in the Table 8.1.

Engine	RPM	Power [HP]	Mass [g]
O.S. [®] 0.55AX	2000 – 17000	1.75	404
Magnum XLS [®] - 61	2000 – 16000	1.90	638

The Table 8.2 is composed by the data gathered in Brazil for the following propellers: *JZ*[®] 13x4, *APC*[®] 13x4, *JXF*[®] 13x6 and *MAS*[®] 13x6. The Figure 8.1 shows the available thrust for each propeller tested varying the speed.

Propeller	13x6	13x6	11x6	11x7
	JXF	MAS	JZ	APC
Rotations [RPM]	9210	8610	10690	12090
Mass[g]	28.7	25	26.8	50.7
Measured Thrust	26 [N]	25 [N]	30 [N]	32 [N]

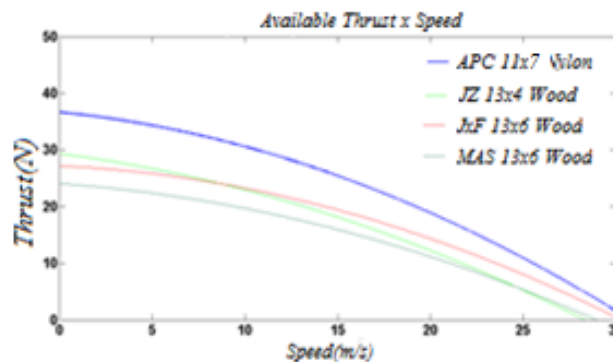


Figure 8.1: Available Thrust vs. Speed

The higher the available thrust of the power plant during the take-off, the higher the payload that can be carried by the aircraft. Understanding this in addition to the experience gained in Brazil, we concluded that the propeller that better suits the project is *APC*[®] 11x7 Nylon sport version.

Having acquired the available and required thrust, we are able to experimentally determine the power at each thrust level. The power curves obtained could be visualized in Figure 8.2. The Figure 8.3 illustrates the relation between thrust and aircraft drag.

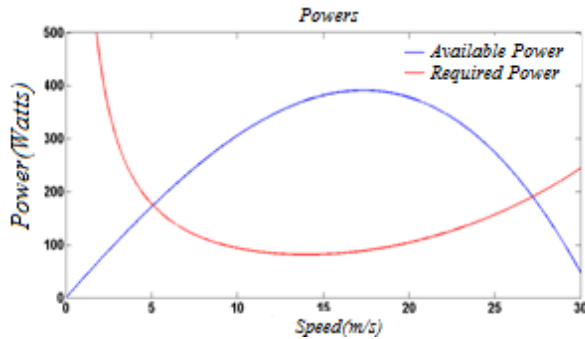


Figure 8.2: Available Thrust and Required Thrust

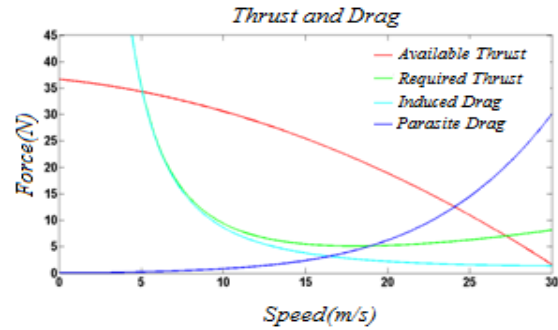


Figure 8.3: Aircraft Thrusts and Drags

8.2 Take-off

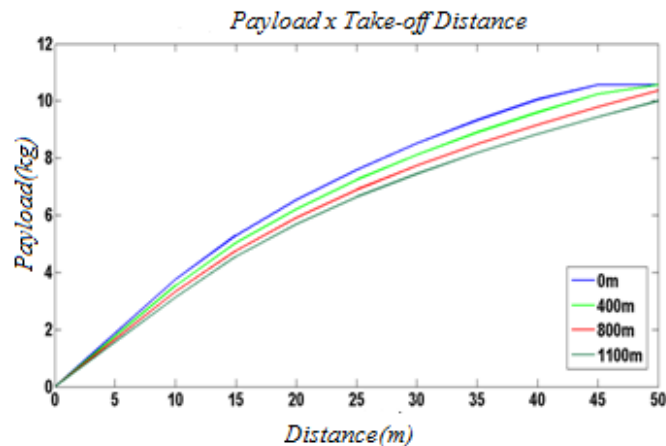
The take-off analysis was based on the method by KRENKEL[18], the numerical adaptations proposed by LYNN [19] and computationally implemented in the *software MATLAB*[®].

The original method by KRENKEL [18] approaches the take-off and climbing phases, but do not take into account the instant that the aircraft rolls. Therefore for higher accuracy in the data obtained, the take-off phase *was included in the calculations according to the methodology proposed by NICOLAI* [20]. The code input data was set for: total take-off distance 50 [m] and the obstacle height in the end of the runway 10 [cm], also the values for C_{Lg} and C_{Dg} were adjusted to ground effect influence based in a study proposed by ROSKAN [6].

In order to evaluate the take-off length required in relation to the payload, a method very similar to the method utilized to calculate the maximum cargo was used, constraining this time the runway length each iteration. Through these means, the relation illustrated in the Figure 8.4 surfaces. The analyses realized were based in the calculations for the following altitude values 0 [m], 400 [m], 800 [m] and 1100 [m].

Table 8.3- Take-off data summary**Carried Payload= 10,000 [kg]**

Take-off Speed	13.42	[m/s]
Obstacle Height	9.98	[cm]
Take-off Total Distance	47.50	[m]
Climb Angle	4.61	[°]
Rate of Climb	1.75	[m/s]
Take-off Time	6.87	[s]

**Figure 8.4: Payload vs. Take-off distance varying altitude**

The data in the Table 8.3 summarizes the main take-off parameters for an altitude-density of 1100 [m]. Lastly, it was assumed that the aircraft achieves take-off after the obstacle height, then it's made possible to validate the procedure.

8.3 Flight Performance

In order to evaluate the flight performance studies were carried out based on the proposals by ANDERSON [7] and ROSKAN [6]. The main speeds are presented in the Table 8.4.

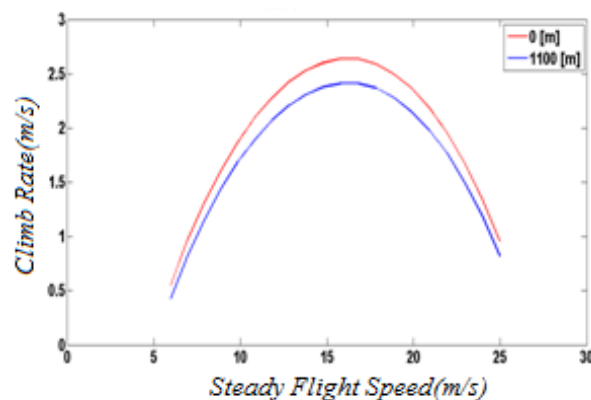
Table 8.4 – Characteristic Speed for 0 [m] and 1100 [m]

	0 [m]	1100 [m]
Stall Speed	10.54 [m/s]	10.86 [m/s]
Maximum Speed	20.56 [m/s]	21.18 [m/s]
Maximum autonomy speed	17.96 [m/s]	18.51 [m/s]
Dive Speed	30.58 [m/s]	30.50 [m/s]

8.4 Climb and Glide Performance

For the climb performance we used an equation that relates the remaining power to your total weight in order to find the rate of climb according to the Equation 8.1. The Figure 8.5 illustrates the climb rate for the altitudes of 0 [m] and 1100 [m]: this confirms the altitude influence in the result.

Parameters	0 [m]	1100 [m]
Maximum Angle of climb	11.03 [°]	9.94 [°]
Speed for Maximum Angle	11.22 [m/s]	11.33 [m/s]
Maximum Rate of Climb	2.68 [m/s]	2.42 [m/s]
Maximum Speed Ratio	16.26 [m/s]	16.19 [m/s]

**Figure 8.5: Climb Rate**

The rate of climb is analyzed for a power cut-off utilizing the Equation 8.2. The Figure 8.6 illustrates the relation between the vertical descend speed and horizontal speed.

Minimum descend angle	2.39 [°]
Minimum angle speed	17.87 [m/s]
Minimum descend	

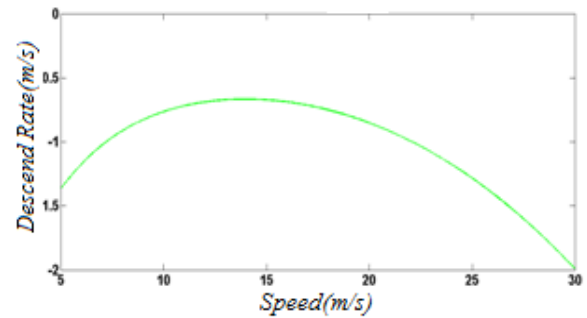


Figure 8.6: Descent Rate

$$R/C = \frac{P_D - P_R}{W} \quad (8.1)$$

$$R/D = \sqrt{\frac{2W}{\rho S (C_L^3 / C_D^2)}} \quad (8.2)$$

8.5 Turning Performance

The study of the turning performance was made according to the methodology proposed by ANDERSON [7] (Equation 8.3 and 8.4). The minimum turning radius was found for a maximum cargo to be 8.48 [m] and an angle for minimum radius of 76.34°. The Figure 8.7 illustrates the total aircraft weight versus turning radius. The Figure 8.8 shows the minimum angle for a minimum turning radius.

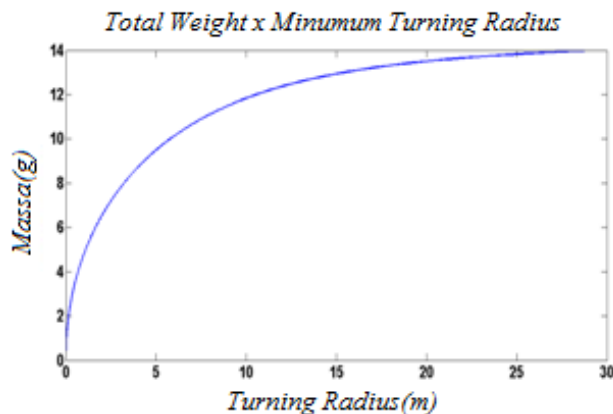


Figure 8.7- Total Weight vs. Minimum Turning Radius

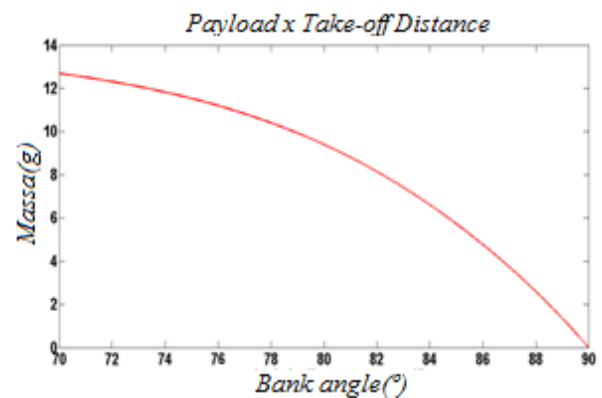


Figure 8.8 – Total mass vs. turning angle

$$r = \frac{4K(W/S)}{g\rho(T/W)\sqrt{1-4KC_{D0}/(T/W)^2}} \quad (8.3)$$

$$\gamma = \tan^{-1}\left(\frac{V_{\max L/D^2}}{gr}\right) \quad (8.4)$$

8.6 Flight Level

In order to calculate the flight level, a routine was implemented in order to obtain an envelopment that is capable to estimate the minimum speed, maximum speed and flight level. In this study the load factor is considered to be $\eta_{max} = 3.8$.

8.7 Landing

In the landing study, the team implemented a routine through the *software MATLAB*[®], using the landing distances developed by RODRIGUES [21] as the basis. The Table 8.7 illustrates the values obtained by this analysis.

	0 [m]	1100 [m]
Landing distance(no brakes are employed)	145.65 [m]	154.63 [m]

50 meters	0.26
75 meters	0.16

8.8 Mission Time

In order to obtain the mission time, every flight phase had its duration calculated (Table 8.10), utilizing the techniques proposed by RODRIGUES [20] and ANDERSON [7], we obtained a total sum of 97.40 [s].

Take-off	6.87 [s]
Climb	17.12 [s]
Turn	26.45 [s]
Descent	40.54 [s]

Consumed Volume	50 [ml]
Consumption Time	233.47 [s]
Average Consumption	0.21 [ml/s]
Total Flight Time (180 cc)	636.93 [s]

Knowing the total mission time and the average consumption it was possible to select the fuel tank that better fits the project. Table 8.10 shows the fuel consumption of the power plant at maximum power. Therefore, the fuel tank selected was a *DUBRO*[®] S-8.

9. LOADS AND STRUCTURE

9.1 Structural Design

During the preliminary analysis, the norm JAR-VLA [12] was extensively used, especially in the estimation of aerodynamic loads and ground loads. In this way, the critical load for each flight scenario was determined. During the detailed design phase the software *Tornado* in *MATLAB*[®] was used to provide the load distribution which in turn was used to size the components.

The softwares *Microsoft Excel*[®], *Ansys*[®] and *CATIA*[®] were used to design the components. In this phase, special care was taken to use failure criterion that better suit the component under study. For the structural design the following references were used BARROS [3] and ISCOLD [13].

9.2 Flight Envelope (V-n)

The V-n diagram was built considering a maximum load factor of $\eta_{max} = 3.8$ and a minimum load factor of $\eta_{min} = -1.5$ for the maneuver envelope, according to JAR-VLA [12] paragraph JAR-337.

The values for minimum, average and maximum speed were used to find the gust values for U_c and U_d , these being respectively $U_c = 2.612$ [m/s] the maximum average speed and $U_d = 1.121$ [m/s] the minimum average speed. The results are show below:

Table 9.1 - V-n Diagram Parameters Flight Envelope		
Maneuver		Gust
$V_c = 24.39$ [m/s]	$U_c = 2.612$ [m/s]	
$V_A = 20.33$ [m/s]	$U_d = 1.121$ [m/s]	
$V_d = 30.49$ [m/s]	Load Factor	
$V_{es} = 10.43$ [m/s]	$n = 3.8$	$n = -1.5$

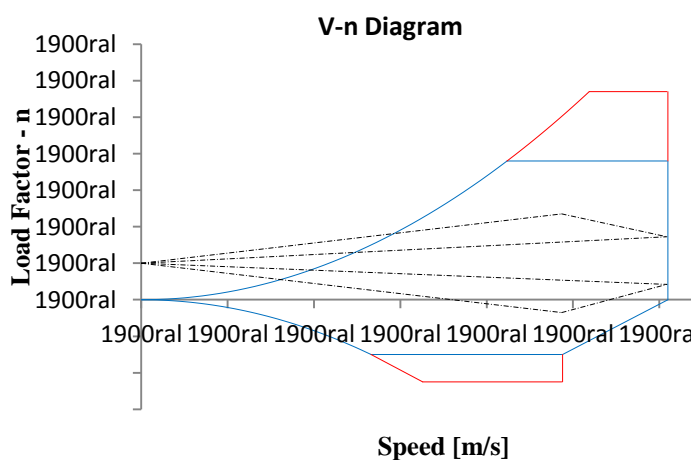


Figure 9.1: V-n Diagram

9.3 Materials Properties

The materials properties were obtained from MATBASE [14] and FOREST PRODUCTS LABORATORY [15].

9.4 Wing Load Determination

The acting stresses were calculated initially with the knowledge of the lifting distribution using the Shrenk method for each flight condition and type of maneuver specified by [12]. The torsion loads were found according to the paragraph JAR-349 and JAR-455. A more depth analysis was performed in the *software Tornado*[®] for a 20° elevator deflection at cruise speed. The load factor reached, under these conditions, is $\eta_{max} = 3.8$. For a critical load on the wing, the results obtained are shown in the Figures 9.2 and 9.3.

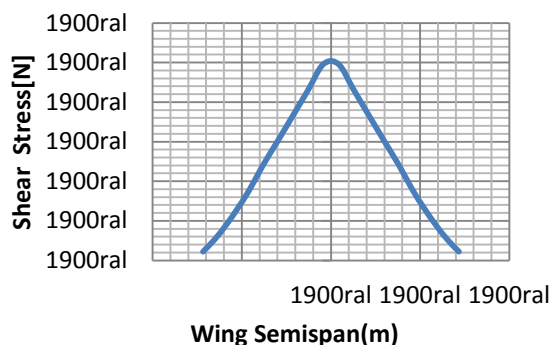


Figure 9.2: Shear Stress Diagram

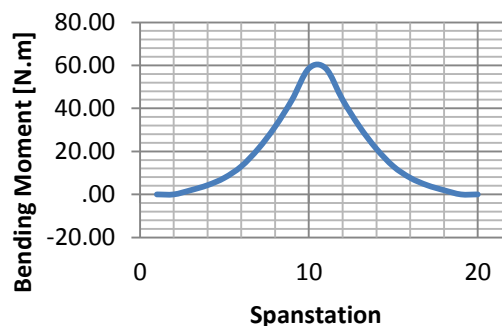


Figure 9.3: Bending Moment Diagram

The center of shear was defined to be 27%; this corresponds to the thickest section of the profile where the pressure center does not change significantly for high angles of attack. Thus, the torsional stress over the spar is reduced significantly.

Several cross section parameters were studied; the polar moment of inertia and the area were the main parameters and the *Microsoft Excel*[®] Solver was used. The constraints were set to be the geometrical limitations imposed by the wing profile, in such a manner to minimize the acting stress in order to respect the total safety coefficient of 1.725, obtained by $(FS)x(FQ)$, with respective values of 1.5 and 1.15.. The final configuration is a rectangular beam made of balsa wood—the geometry that presented the highest $(J/S)_{lg}$ ratio.

Aero-elasticity effects were considered due to the high aspect ratio of the wing, the failure criteria was defined as follows: the wing tip cannot exceed 2°; this value was chosen in order to avoid an aileron stall. In the test shown in Figure 9.2, the angle calculated was about 0.73°, considering the situation of a take-off roll, generating a maximum force on the ailerons equal to 16.0 [N], as calculated in the Stability and Control analysis.

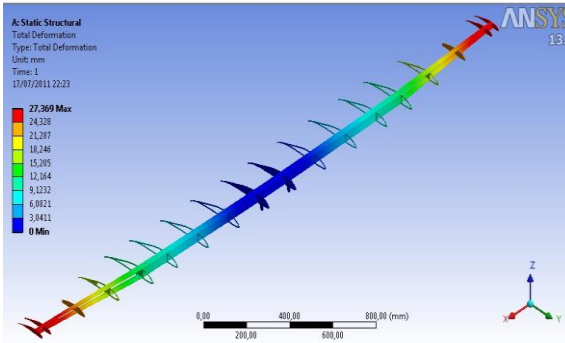


Figure 9.4: Bending Analysis

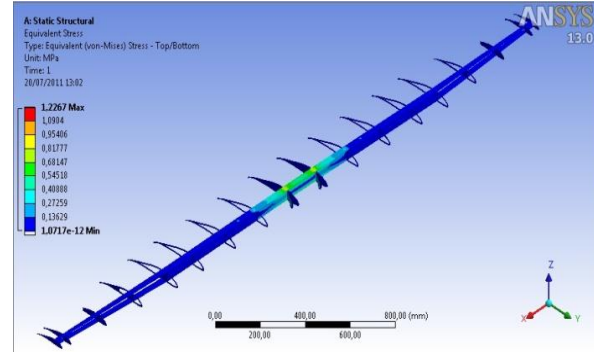


Figure 9.5: Torsion Analysis

9.5 Front Wheel

The aluminum alloy AA 6061-T3 was chosen. On the drawing in annex number 2, one can find the front wheel drawing. Its 60° rotation movement is possible due to low friction between the UHMW components.

9.6 Landing Gear

The landing gear design was aimed to provide the minimum weight possible and maximum performance to the situation indicated by the JAR-VLA [12]. The configuration was obtained considering mainly the CG location and load distribution between the main wheels and nose. According to RAYMER [1] the turnover angle was obtained and the distance between wheels was calculated.

According to the JAR-VLA [12], the ground factor was set to $\eta_g = 2.67$, calculating a maximum admissible reaction force $R_{max} = 325.3$ [N], given by the Equation 9.1.

$$n_g = \frac{R_{max}}{W} \quad (9.1)$$

The maximum speed that the structure can resist without touching the ground was calculated considering that at the maximum deflection point there is no kinetic energy, only potential energy. Equating the initial energy to the energy stored due to the deflection, one can obtain the Equation 9.2.

$$\frac{1}{2g} V_{dc}^2 = (n_{rd} \cdot n_g \cdot \Delta_{rd}) + (n_{tp} \cdot n_g \cdot \Delta_{tp}) + \Delta_{rd} (k_L - 1) + \Delta_{tp} (k_L - 1) \quad (9.2)$$

Considering that the wheels do not undergo deflection, one can adopt Δ_{rd} as zero. Therefore, the maximum descent speed is 0.72 [m/s].

In order to reduce the bending without increasing the component weight and increase the section inertia moment of the cross section, an initial model was designed in CAD and its stress distribution was found using the FEM code embodied in CATIA, and the design was optimized. It was possible to achieve a weight reduction of 42 g. without changing its maximum deflection of 2%.

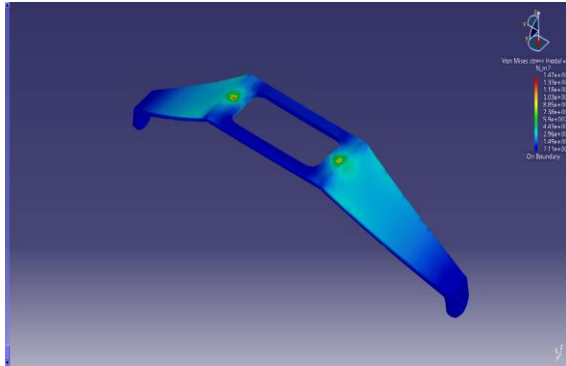


Figure 9.6: Landing Gear I

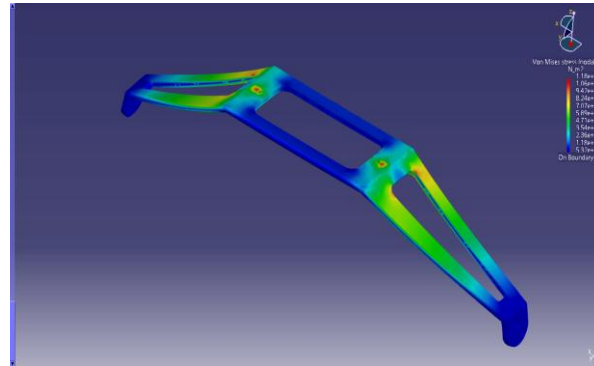


Figure 9.7: Landing Gear II

Several types of landing were considered to validate the aircraft to all possible landing configurations.

9.7 Level Landing

In order to calculate the energy absorbed at the moment that the front and main landing gear touch the ground, we apply the Equation 9.3. Since both gears touch the ground at the same time in this type of landing, it is important to present the total energy as the energy they must absorb.

$$E_{tp} + E_b = \frac{W \cdot v_{dc}^2}{2 \cdot g} \quad (9.3)$$

By mean of the above calculation, one obtains 3.25 [J] as the total energy absorbed and by the JAR-VLA 479 calculation, E_{tp} represents 75% and E_b 25% of this value. Comparing $E_{tp} = 2.03$ [J], generated by the descend ratio calculated in the previous sections with $E_{tp} = 2.44$ [J], from the Equation 9.3, validated the landing gear sizing.

9.8 Landing on Two Main Gears

The angular acceleration during a pitch maneuver generates an apparent weight on the centroid, which can be evaluated by the Equation 9.4

$$W' = \frac{W}{1 + \frac{I_{CG} \alpha^2}{k_y^2} + \frac{c_{at} \cdot h_{CG} \cdot I_{CG}}{k_y^2}} \quad (9.4)$$

9.10 Wing

Each wing semispan was divided into sections in order to calculate the load distribution according to the methodology presented by BARROS [3], the results are summarized below.

Two tests were realized, one with negative bending and the other with positive bending, representing a landing situation and an in-flight situation respectively.

Table 9.3 - Percentage of applied load in each sector in relation to the total load applied on the wing semispan

Sector	1°	2°	3°	4°	5°	6°	7°	8°	9°
Percentual (%)	18	16.5	15.5	14.5	13	10	7	3.5	2

Table 9.2 – Bending recorded after the load in each wing semispan

Load	60,9 [N] (1)	91,4 [N] (2)
Negative bending	26 [mm]	42 [mm]
Positive bending	25 [mm]	34 [mm]

Analyzing the Table 9.3 and comparing it with the computational tests, we conclude that under critical flight conditions, the spar will resist the acting loads.

9.11 Landing Gear [Model]

According to ISCOLD [13] and the norms JAR-VLA 723-725 [12], we were able to determine the bending caused by the calculated ultimate load. To do so, static tests were made on the landing gear by applying loadings until the limit, 121.8 [N]. The obtained maximum strain was about 2.5 [m].

9.12 Wheels

The team observed that wheels made in nylon UHMW present high shock resistance, low weight and a friction coefficient that suits the project requirements. For mass reduction only one bearing was used in each wheel and relief holes were made.

9.13 Aircraft Empty Weight Estimation

The team placed utmost importance on the weight estimation since this has a major impact on the performance characteristics and maximum payload to be carried. In order to preview the empty weight, the team has determined the density of all the materials employed. These values

were inserted in the software *CATIA*[®], some optimization was carried out in an overall aspect of the aircraft in order to reduce its gross empty weight.

10. Electrical and Electronics Design

10.1 General Considerations

Analyzing past designs we could conclude that several components were oversized adding extra mass which is undesirable for the project conclusively. This year, we aimed at a maximum weight reduction component by component without interfering with the aircraft controls.

10.2 Radio, Receiver and Servo Selection

The team is using an *AR115 six Channel DSMX Microlite Spektrum*[®] receiver. The receiver is placed on the tail in order to positively affect CG location.

The aileron and the rudder are actuated by the servos *Hobbico*[®] CS-35MG and *Hobbico*[®] CS-12MG respectively, which present more than adequate amounts of torque and metal gears that are highly resistant to shock yielding safer flight of the aircraft. For the engine the servo *HXT-900* was used. For the front gear the team has opted for the servo *Hobbico*[®] CS-35MG. The elevator uses a servo *Hobbico*[®] CS-64MG.

Table 10.1 – Characteristics of Servos Utilized

Servo	Qtd.	Component	Voltage[V]	Labeled Torque [kg.cm]	Real Torque [kg.cm]	Mass [g]
HXT-900	1	Motor	4.8	1.6	1.5	9.0
CS-64	1	Elevator	4.8	5.0	4.9	50.0
CS-12MG	1	Rudder	4.8	2.6	2.5	19.0
CS-35MG	3	Aileron and Steering Wheel	4.8	3.2	3.0	28.0
Total	6	-----	-----	-----	-----	162.0

10.3 Electric Wire and Power Demand

The highest current consumed by a servo in the circuit is 1.51 [A]. Establishing 24.5% of safety margin in the maximum current supported, we calculated, according to the pattern AWG, a new size for the wiring harness cables: 24 gauge [AWG] which support a maximum current of 2 [A].

The Figure 10.2 shows a plot of current in function of time in the servo CS-64 and CS-12, where the vertical axis represents the current in ampere and the horizontal axis stands for time.

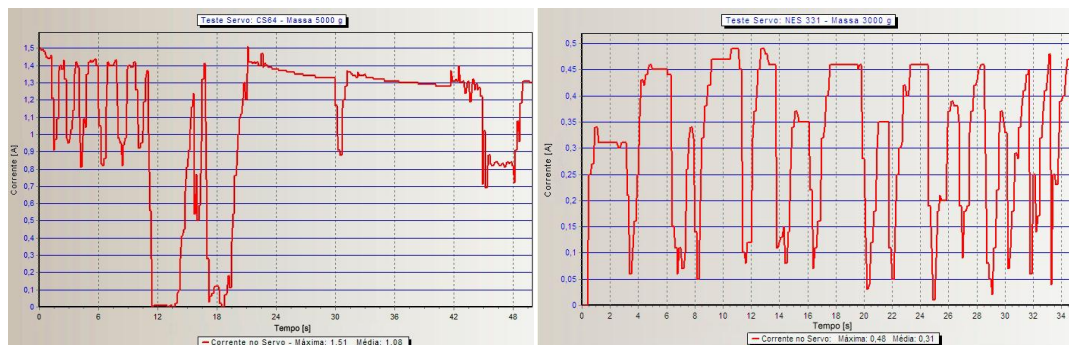


Figure 10.1: Electrical current in function of time in the servos CS-64 and CS-12

10.4 Battery and Demand Charge

The battery utilized is *SMC Lightning Volts*[®] SUM1650ML composed of *Li-Po*. Its characteristics are shown in the Table 10.2. Its mass/power ratio is excellent and its recharge time when compared to other batteries is mediocre.

Considering a one minute time interval for the take-off and landing, and about 7 minutes for the flight loft, we obtained the Table 10.3.

Table 10.2 – Battery specifications

Battery	Li-Po
Charge	1650 [mAh]
Number of cells	2
Nominal Voltage	7.4 [V]
Maximum discharge current	8000 [mA]
Mass	84.5 [g]

Table 10.3 – Current demand

Component	Quantity	Consumed Load [mAh]
CS-12MG	1	78.49
CS-35MG	3	255.47
CS-64MG	1	153.81
HXT-900	1	51.27
Receiver	1	1.87
Total		540.91

According to BOYLESTAD [17], and considering a 20% safety margin on the load caused by the electrical components, we obtain a load consume of approximately 650 [mAh]. The battery utilized provides 1650 [mAh], sufficient load to supply the necessities of this project.

10.5 Voltwatch and Voltage Regulator

The voltwatch selected is a Li-Po battery measurer; it is placed on the aircraft tail, to be located closely to the receiver and the battery. In order to reduce the voltage from 7.4 [V] to approximately 5.0 [V], a *FlightPower*[®] FT8AVR voltage regulator is utilized according to the Table 10.4, connected in series with the battery.

Table 10.4 – Voltage regulator specifications

Input Voltage	6.0 [V] to 8.4 [V]
Output Voltage	5.0 [V] to 6.0 [V]
Current	0 to 5.0 [A]
Mass	53[g]

10.6 Electrical Diagram

The **Error! Reference source not found.**3 shows the basic electrical schematic and the connection of the servos, battery, voltmeter, switch and the voltage regulator into the receiver.

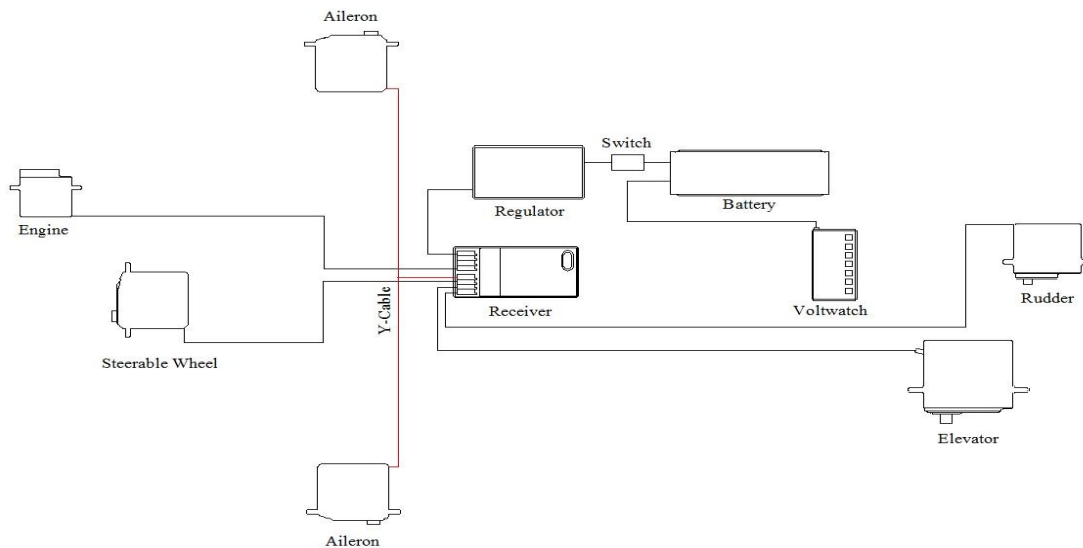


Figure 10.3: Electrical Diagram

11. Environment, Health and Safety

11.1 Environment

Balsa wood comes from the fast growing balsa tree which is native to Central and South America. The wood's environmental impact is minimal due to the nature of the supplier. Midwest Products gets the Wood from suppliers who grow balsa tree farms, and do not harvest naturally growing trees. If desired, the wood can be recycled for future use in model fabrication or burned in a wood pellet furnace and converted to energy. The method of delivery for balsa wood has the most negative impact on the environment due to its long distance of travel.

11.2 Health

The fast drying glue used during construction is difficult to avoid coming into contact with one's skin. Although this fact is forewarned on the label, the only minor health issues to come from this were the loss of first layers of skin. When using accelerator to quickset the glue, the chemical reaction between the glue and accelerator could cause minor burning if skin contact is made with the glued surface. The fuel used to in the R/C engine is nitro-methane and is

generally not harmful to humans under short exposure. Ingesting or inhaling too much may induce vomiting.

11.3 Safety

At all times, one should be aware of their surroundings and especially their location in regards to the motor. At full speed, the motor can spin the propeller at 16,000 RPM. This is a high enough velocity to take off a finger of an adult. Protective gloves should be worn if making modifications to the throttle body manually. Glue should be kept away from eyes and never ingested. If either occurs, consult a physician.

12. Conclusions

The aerodynamic design was guided mainly by two aspects: the lift necessary to carry the payload and aerodynamic efficiency. The aircraft stability for longitudinal, directional, and lateral modes were evaluated. The following dynamic stability modes were analyzed: longitudinal, directional and lateral. Lateral-directional control calculations were also done and helped us to size the rudder. The aircraft is considered to be stable and controllable under all of the aforementioned modes. The weight estimation method is considered reliable. In the electronic design, servos were tested and the according plots were constructed. The structure was designed to combine structural integrity with low weight. Environment, Health and safety considerations were made. The team believes that the aircraft has satisfied the mandatory requirements as well as the first two objectives. Our pilot has not been able to conduct a test flight so far and the competition on April 28th has not occurred thus far and therefore our placing is yet to be determined. Also, to ensure our opportunity to place at the competition a second plane will be constructed given time to do so.

13. Acknowledgements

We would like to take the time to give our gratitude to a few people who have helped us in growing as future engineers and have given valuable advice as well as help when needed. Thanks to **Dr. Chiang Shih** for being our project's advisor and pledging to come to competition with us. Thanks to our professors **Dr. Srinivas Kosaraju** and **Dr. Matthieu Dalban-Canassy** for guiding our project in the correct direction during staff meetings as well as being flexible on those meetings' time so that we could all attend. Thanks to **Tony Arnaoutis** for volunteering to be our pilot so that we don't have to deal with utilizing a random pilot at the SAE competition. We would also like to thank him for his multiple drives to Tallahassee to give advice on various construction methods of the plane and to help break in our engine. Thanks to the employees at **Hobbytown USA Tallahassee** for being our go-to guys for all our parts and needs as well as being flexible when it came to dealing with John Cloos and payments from the financial department.

14. International Experiences

The experiences shared by this team are incomparable to those of other design teams this year. The knowledge obtained from the success of an international exchange of students between universities developed our team into an international collaborative effort to succeed from a distance. One of the most significant aspects brought forth by the exchange were the obstacles faced in communication whether it be language barrier or transmission of project headway – a problem not too common amongst all other teams working as a unit together in one place at the same time.

The entirety of the first semester the team was separated by a few thousand miles of ocean and hours difference in time zone. The key factor which had to be understood and overcome was the need for clear and effective communication. This led to a means of finding alternatives to face-to-face communication and with current technologies it was easily solved with the help of the internet; more specifically FaceBook and Skype to communicate and share ideas, pictures, drawings, etc. Unfortunately, even the advanced technology was not enough to overcome the separation, which led to difficulties in assessing contributions of each team member. The lack of understanding did not diverge the team from its goals and the Brazilian students in Tallahassee informed the less experienced students who remained of their knowledge and worked together, while the students studying abroad in Brazil were actively involved with the construction of an aircraft for competition with the aerodesign team, Uirá, in Brazil.

Cultures differences also brought about a unique dynamic throughout the course of our design project as ways of thinking and experiences affected the methods and techniques during the construction process. An obvious aspect would be the language barrier; which slowly dissipated as exchange teammates grew more knowledgeable and more comfortable with the Portuguese language with their time spent in Brazil. Also, the local American portion of the team developed a tighter bond with their teammate(s) from Brazil.

Overall, the international collaborative proved to be a challenge initially however a much needed exposure to working on projects where you are not necessarily always within the same realm physically and/or culturally provided an idea for the team as to how one can avoid problems in the future if ever put in a similar situation. The project resulted in a success and given the opportunity the participate definitely gives our team an edge both compared to other design teams and in the industry where we will all find ourselves solving problems in the future.

15. Appendix – Supporting Software Descriptions

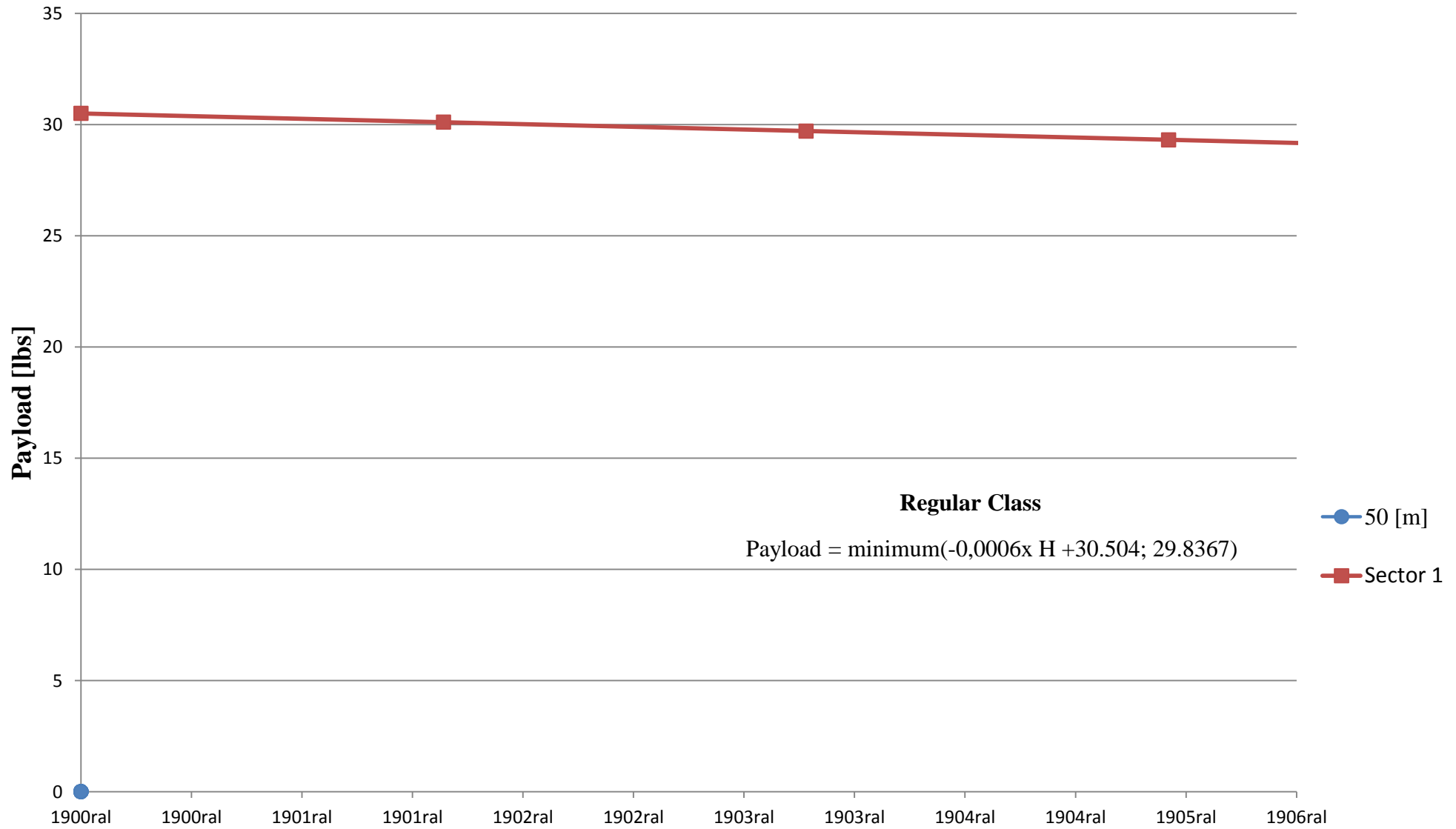
XFLR5: is an interactive program for the design and analysis of subsonic isolated single-segment airfoils . Also is free airplane design software to solve computations for preliminary Aircraft Design, Wing & Aircraft Aerodynamics, and Aircraft Stability. It uses a code written at MIT by Professor Mark Drela and adds a graphical user interface for Windows operating systems. XFLR5 also offers a 3D wing design capability, using two different calculation methods: a Vortex Lattice Method and The Lift Line Theory (LLT). It also can perform a 3D panel analysis for an entire aircraft. The airfoil module can generate 4 or 5 digit NACA airfoils internally or generate any airfoil in .dat format. The data can be displayed in standard performance graphs and the user can compare several airfoils or the user can specify the variables to be graphed. The pressure distribution, streamlines and other parameters are similar to results from expensive CFD software. The code is intended for linear aerodynamic wing design applications, in conceptual aircraft design or in aeronautical education. Among other things it can perform computing and displaying the Trefftz plane velocity vector field.

AVL: Athena Vortice Lattice Method is a program for the aerodynamic and flight-dynamic analysis of rigid aircraft of arbitrary configuration. It employs an extended vortex lattice model for the lifting surfaces, together with a slender-body model for fuselages and nacelles. General nonlinear flight states can be specified. The flight dynamic analysis combines a full linearization of the aerodynamic model about any flight state, trim calculation and dynamic stability analysis, together with specified mass properties.

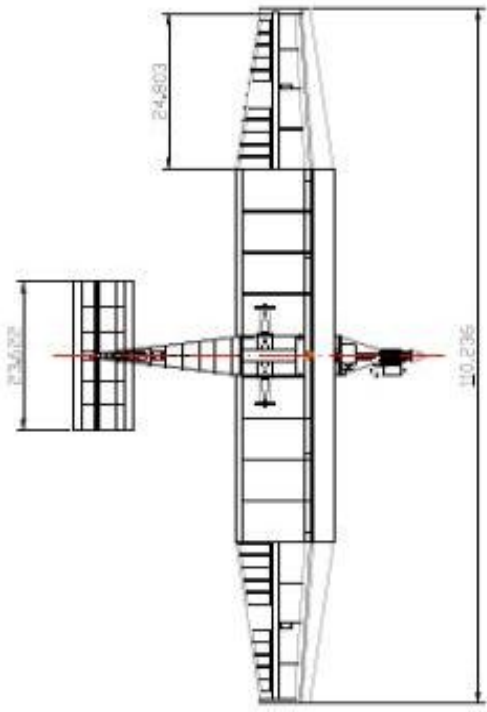
CATIA V6: puts 3D collaborative innovation at the heart of the enterprise and helps accelerate companies' transformation toward a full PLM 2.0 approach. Going far beyond traditional CAD software tools, CATIA V6 offers a unique digital product experience that brings 3D product design to life with unmatched realism. Thousands of companies in multiple industries worldwide have taken advantage of CATIA's virtual design capabilities to ensure product success. CATIA design software delivers products and solutions for the companies of all sizes, from large enterprises and small and medium businesses.

Florida State University: The Flying Spear – Tallahassee, FL

Payload Graph

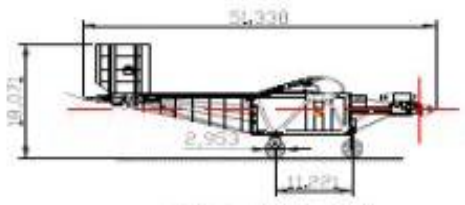
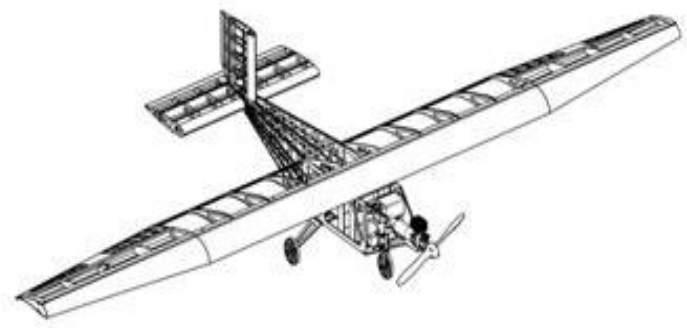


16.Engineering Drawings



Top View

✦ C.G Location



Right Side View

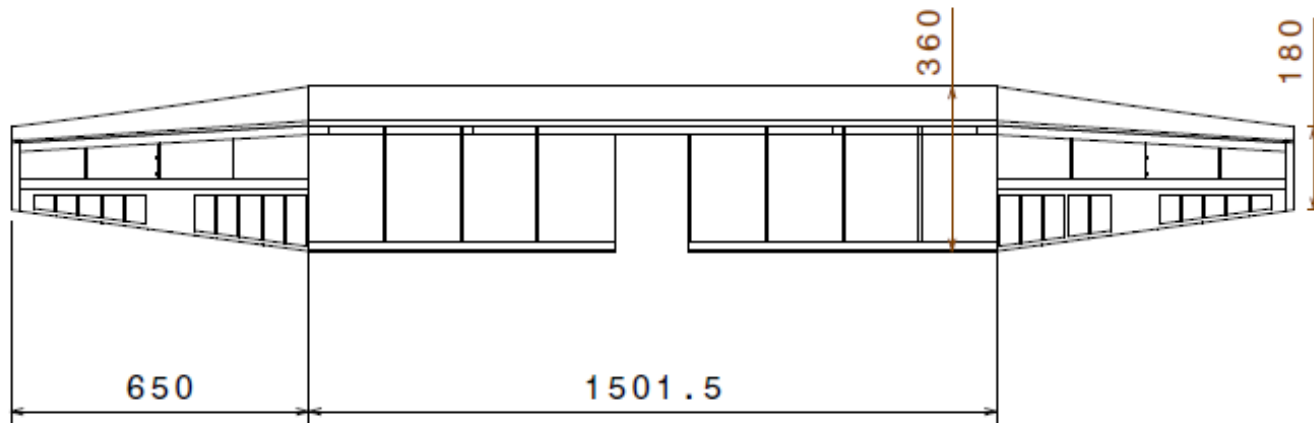
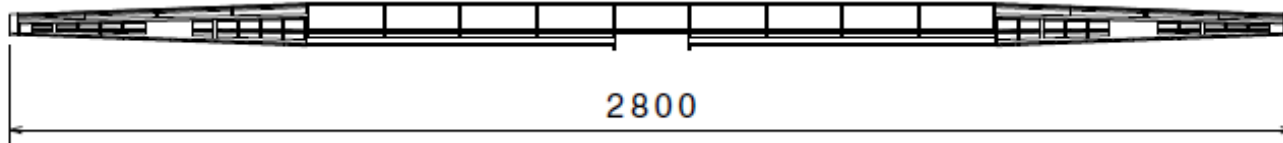
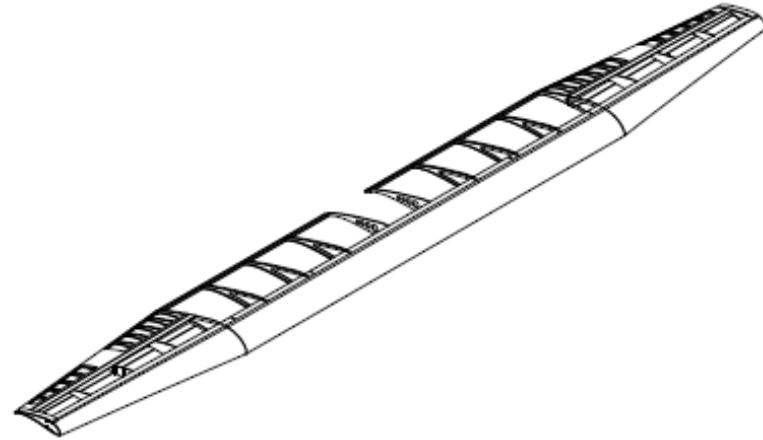


Front View

The Flying Spear		
Main Dimensions (in)		
L	Length	51,338
H	Height	18,071
B1	Wingspan	110,236
B2	Elevator span	23,622
Total		203,267
General Characteristics		
Wing		
Wing Area (in ²)		1302,003
Aspect Ratio		10,5
Profile		Uir41540
Horizontal Emp.(EH)		
Area (in ²)		204,600
Aspect Ratio		3,3
Profile		NACA-0016
Volume Coef.		0,25
Vertical Emp. (EV)		
Area (in ²)		62,001
Aspect Ratio		1,6
Profile		NACA-0016
Volume Coef.		0,035
Empty Weight		3,000 kg

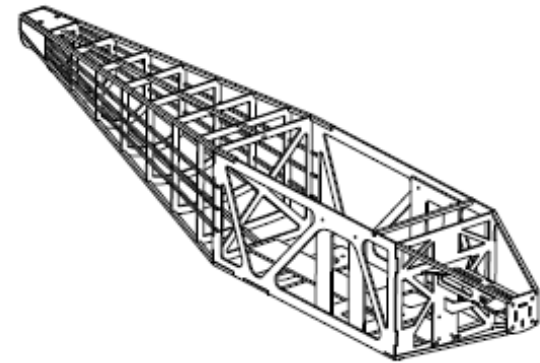
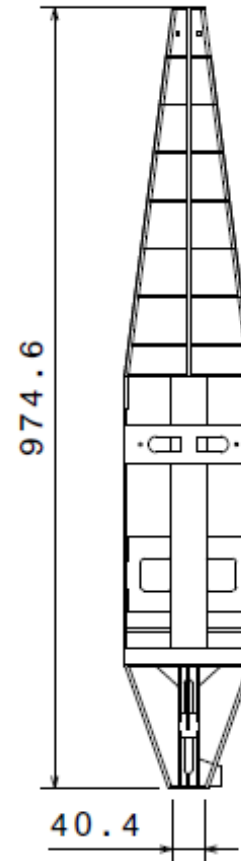
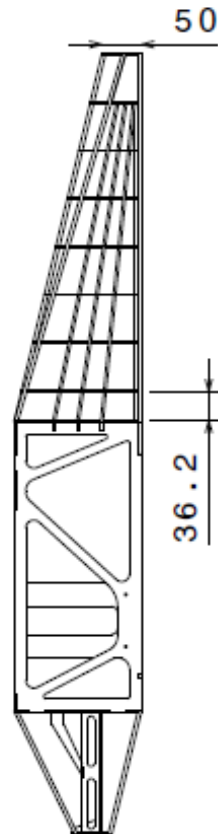
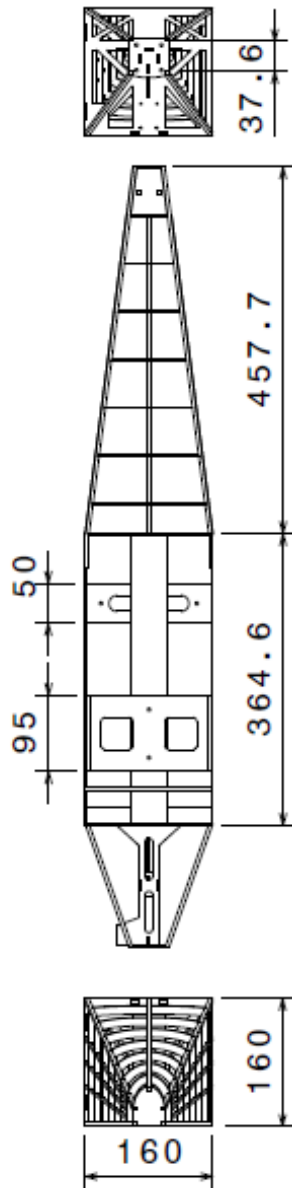
THE FLYING SPEAR TEAM - 039			
Florida State University			
FAMU-FSU College of Engineering			
SAE Aero Design® East - 2012			
Autors:	Design:	The Flying Spear Team	
Three Views		Sheet Plant n°:	1/2
		Scale:	1:18
Date:	03/07/2012	Unity:	in

The Flying Spear 039



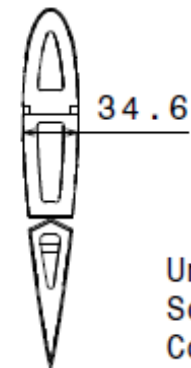
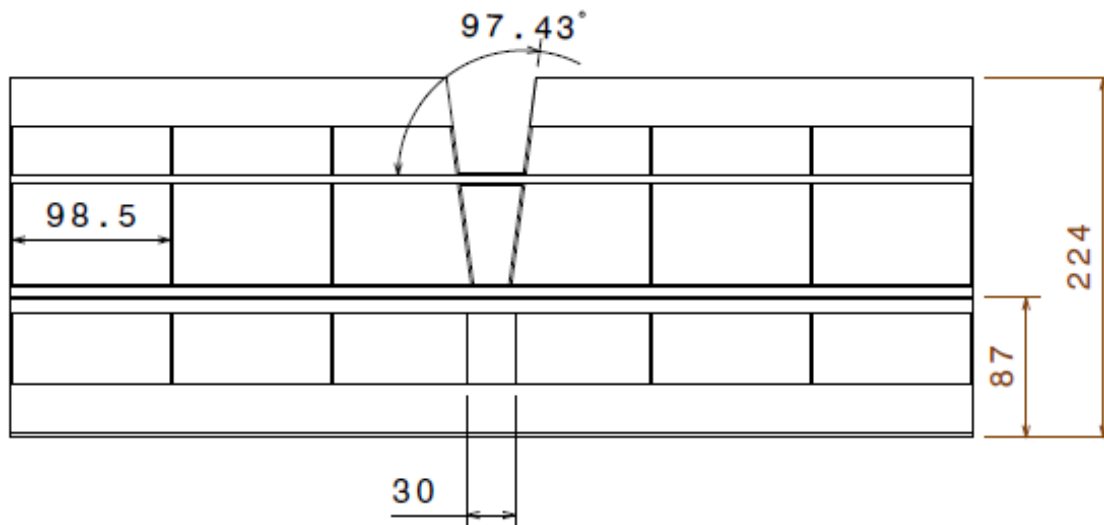
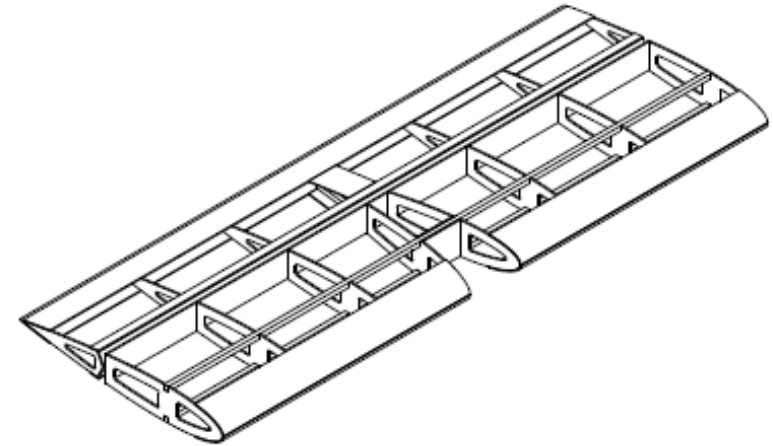
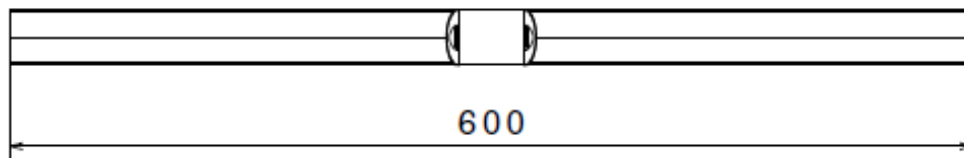
Unit: mm
Scale: 1:14
Component: Wing

The Flying Spear 039



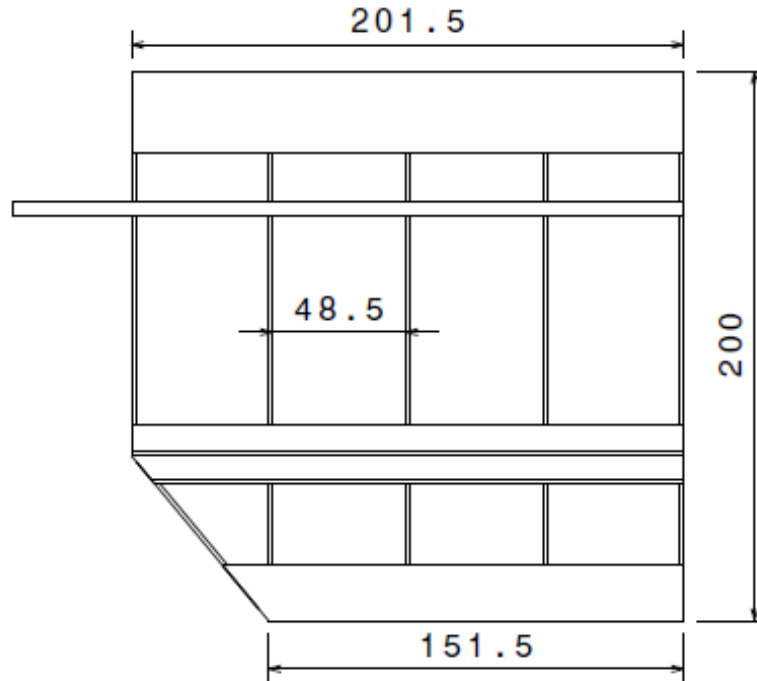
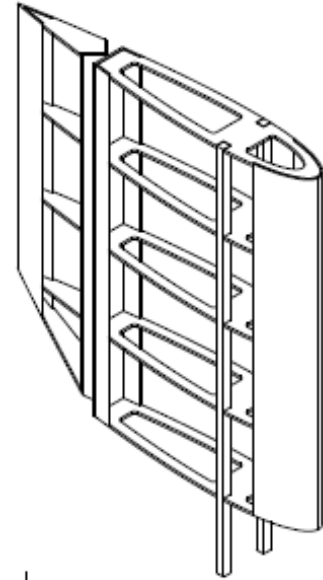
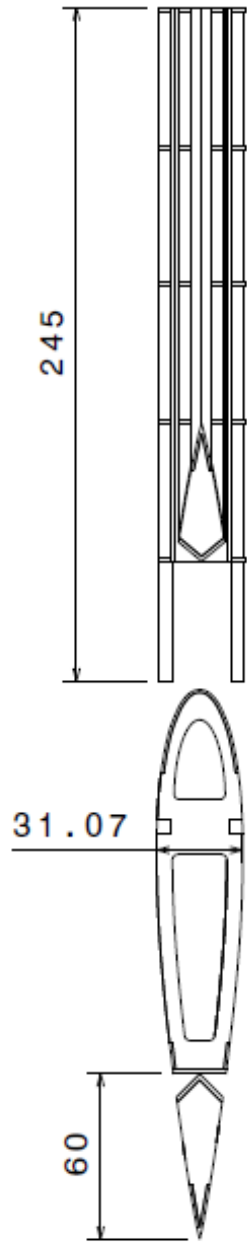
Unit: mm
 Scale: 1:8
 Component: Fuselage

The Flying Spear 039



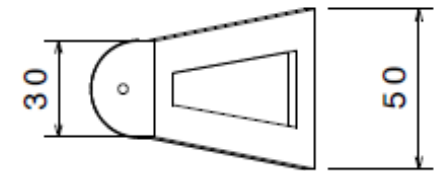
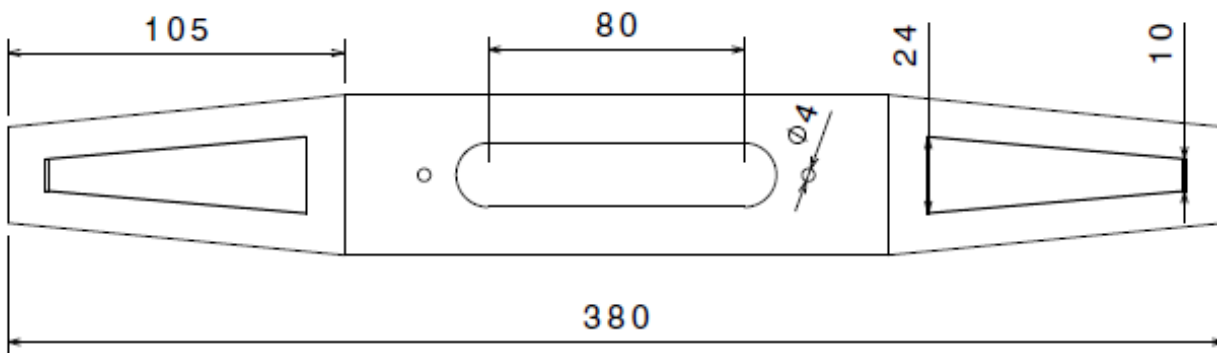
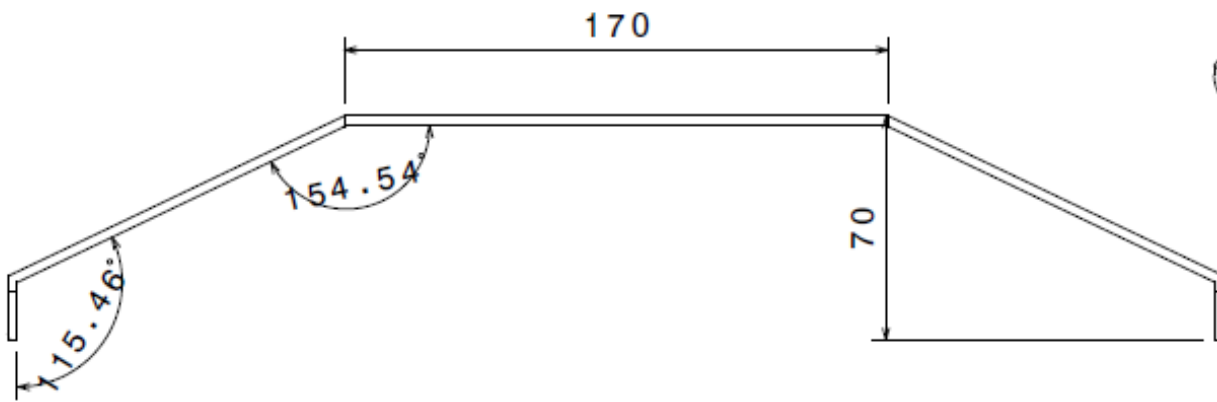
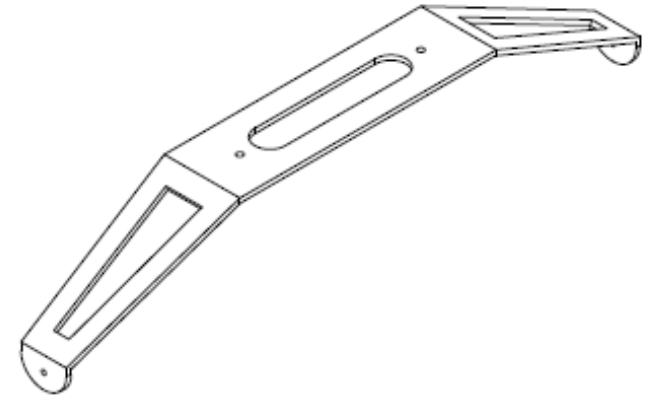
Unit: mm
Scale: 1:3
Component: Horizontal Stabilizer

The Flying Spear 039



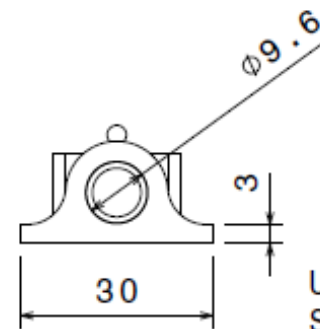
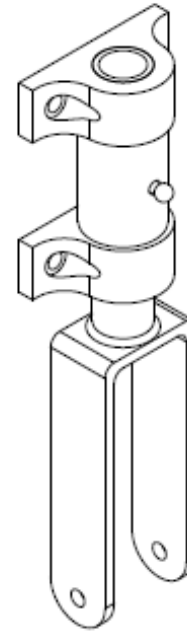
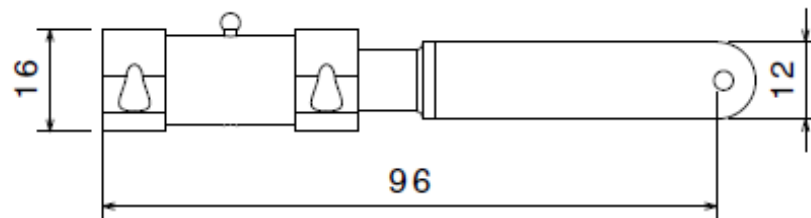
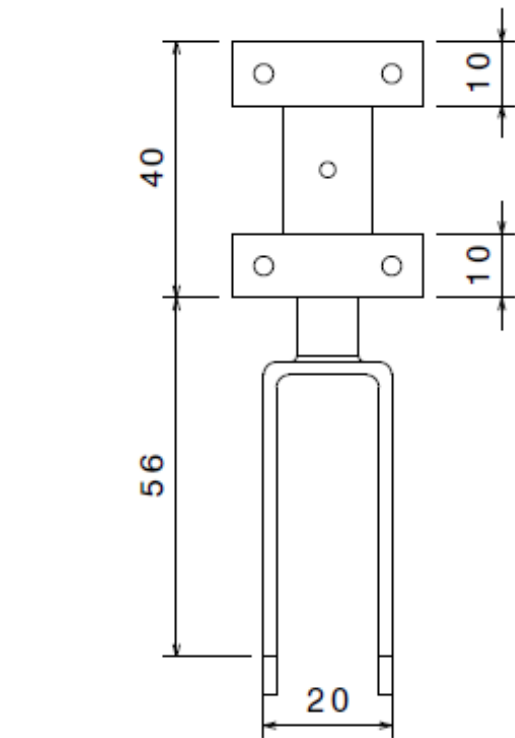
Unit: mm
Scale: 1:3
Component: Vertical Stabilizer

The Flying Spear 039



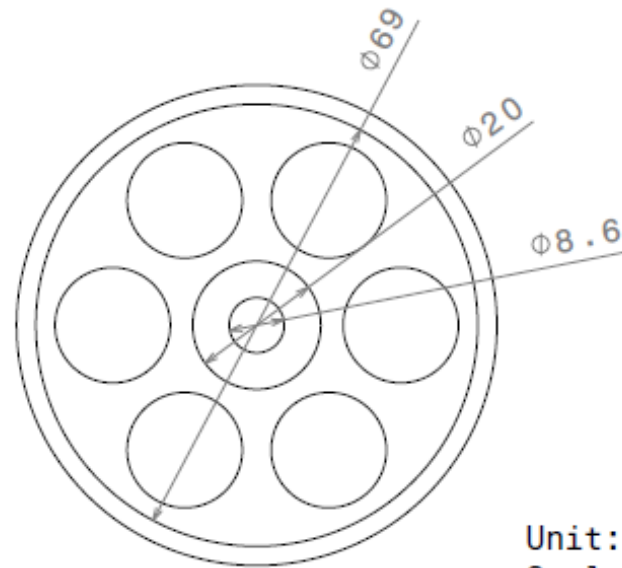
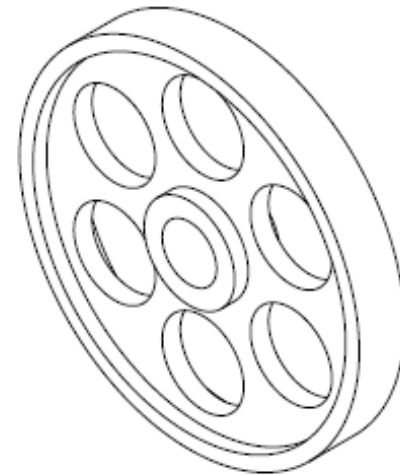
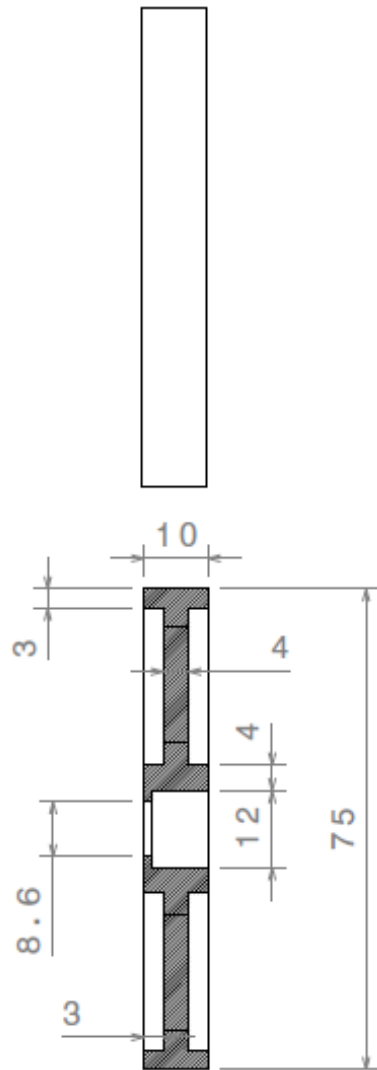
Unit: mm
Scale: 1:2
Component: Landing Gear

The Flying Spear 039



Unit: mm
Scale: 1:1
Component: Steerable Wheel

The Flying Spear 039



Unit: mm
Scale: 1:1
Component: Wheel

17. References

- [1] ABBOTT, I.; VON DOENHOFF, A. *Theory of Wing Sections*. New York: McGraw-Hill, 1949.
- [2] ANDERSON JUNIOR, J. *Aircraft performance and design*. New York: McGraw-Hill, 1999.
- [3] ANDERSON JUNIOR, J. *Introduction to flight*. New York: McGraw-Hill, 2005.
- [4] CORKE, T. *Design of aircraft*. Upper Saddle River: Prentice Hall, 2002.
- [5] FONSECA, A. *Curso de mecânica*. 3. ed. Rio de Janeiro: Livro Técnico, 1972. 4v.
- [6] HAGE, R.; PERKINS, C. *Airplane performance stability and control*. New York: John Willey and Sons, 1949.
- [7] ISCOLD, P. *Introdução às cargas nas aeronaves*. Material didático instrucional do Centro de Estudos Aeronáuticos. Universidade Federal de Minas Gerais, Belo Horizonte, 2002.
- [8] JOINT AVIATION AUTHORITIES COMMITTEE. *Joint Aviation Aircraft: very light aeroplanes*. Netherlands: JAA, 1990.
- [9] KRENKEL, A.; SALZMAN, A., *Takeoff Performance of Jet-Propelled Conventional and Vectored-Thrust STOL Aircraft*, Journal of Aircraft, v. 5, n. 5, 1968.
- [10] LAU, F.; OLIVEIRA, J. Licenciatura em Engenharia Aeroespacial: semestre de primavera 2004/2005. Disponível em: <http://www.dem.ist.utl.pt/~m_ev/#infor>. Acesso em: 10 jul. 2009.
- [11] MATBASE: a leap forward in material data. Disponível em: <<http://www.matbase.com/>>. Acesso em: 20 jul. 2009.
- [12] MEGSON, T. *Aircraft structures for engineering students*. 3. ed. Amsterdam: Elsevier, 1999.
- [13] RAYMER, D. *Aircraft Design: a conceptual approach*. Washington: AIAA Education Series, 1992.
- [14] ROSA, E. *Introdução ao projeto aeronáutico: uma contribuição à competição SAE AeroDesign*. Colaboração de Juliano Toporoski. Florianópolis, USFC/GRANTE: Tribo da Ilha, 2006.
- [15] ROSKAN, J. *Airplane Design: part IV – preliminary calculation of aerodynamic, thrust and power characteristics*. Lawrence, University of Kansas: AIAA Education Series, 1990.
- [16] SCHLICHTING, H.; TRUCKENBRODT, E.; RAMM, H. *Aerodynamics of the Airplane*. New York: Graw-Hill, 1979.

[17] TORENBEEK, E. *Synthesis of subsonic airplane design*. 2 ed. Rotterdam: Nijgh-Wolters-Noordhoff, 1976

18. Biographical Sketch

The 2012 FSU Flying Spear team is a single disciplinary, multicultural team combining talented young men from both Florida State University and Universidade Federal de Itajubá located in Minas Gerais, Brazil. It will be the first team from Florida State University to compete in SAE's Aero Design East competition and are paving the way for future students at the University to compete as well as providing a launching point for future design teams. The standard design constructed by the team is complex by design and complicated to construct. Every member has been on the team all year, except Eduardo Krupa who joined the team this January. Eduardo has proven invaluable to the team in his knowledge of building while his brother Gustavo has been equally invaluable at understanding small aircraft design methodology. This has helped the rest of the team follow in suit in understanding conceptual design, implementation, and construction phases. The Flying Spear is very anxious to attend the competition in Marietta, Georgia the weekend of April 27th.

Eduardo Krupa was born in Itajubá, Brazil in 1990. At 18 he went to study mechanical engineering at Universidade Federal de Itajubá (UNIFEI). At this college he began to explore his interest in designing aircrafts when he entered to the Uirá, a team that participates at SAE Brazil Aero Design competition. He served as Team captain, Structures & loads leader and aerodynamicist developing skills with CAE tools, leadership and logistics. Now he is studying at Florida State University through an exchange visitor program between the universities. His major interests are UAV/UCAVs systems, aircraft design and military sciences.

Gustavo P. Krupa was born in São Paulo, Brazil. He started to study mechanical engineering at UEM (Universidade Estadual de Maringá) in 2008. In 2009, he applied to UNIFEI (Universidade Federal de Itajubá). At UNIFEI, he joined the UNIFEI Aero Design team called Uirá working in the field of aerodynamics. In 2011, being part of the CAPES/FIPSE program between UNIFEI and Florida State, he joined the Aero Design team of Florida State. His main interests are computational fluid dynamics, continuum mechanics and aerospace sciences.

David L. Williams was born in Key West, Fl. He became interested in mechanical engineering when he got his first car and began working on it himself. He began studying at Florida State University in 2006 but did not become a mechanical engineer major until his sophomore year. This is his first hands on experience working with aeronautical concepts,

building, and design, but has always had a strong interest in the field. He holds two minors, math and physics, and has also taken many economics classes. In the field of engineering, his main areas of studies have been material science, thermo-fluid design, and sustainable energy.

Jordan Taligoski is a Florida native; born and raised in Hollywood, Florida. He began attending Florida State University after graduating from South Broward High School in 2007, selecting Mechanical Engineering as his intended major after discovering his curiosity in how things work and renewable sources of energy. In 2011 he was admitted into the FIPSE exchange with Brazil and began learning Brazilian Portuguese, where he mastered the language after the exchange in fall 2011. Attending UNIFEI secured his participation on Team 10-SAE Aerodesign when he studied and participated in team Uirá at UNIFEI. His principle interests in Mechanical Engineering involve thermodynamics, propulsion systems and sustainable energy.

Dimitrios Arnaoutis was born in Daytona Beach, FL in 1989. His father taught him to build and fly model R/C airplanes at a young age. He also has had an interest in cars and motorsports from an early age. This interest directed him to the field of mechanical engineering. Accordingly, during registration for Florida State University the mechanical engineering track was chosen. He then became a member of the Society of Automotive Engineers and participated in the Formula SAE team. He still has a strong interest in automotive suspension and power train design.

Alessandro (Alex) Cuomo was born in Hartford, CT in 1990. Weeks later his family moved to Huntington Beach, CA where he spent most of his childhood before moving to Florida in 2002. The latter years of high school motivated him to pursue a college education in the science and mathematics field. In 2008, Alex came to Florida State University and entered as a freshman in the exploratory major. Seeking advice from a personal coach, Adrian Husband, he was able to pave the way into the engineering school to start a career in mechanical engineering. In the fall of 2011, he participated as part of the inaugural group of students sent to Brazil in a mechanical engineering foreign exchange under the FIPSE program. Through the experience in the program and elective courses he pursued in his career at FSU he has developed interest in the sustainable energy field, thermodynamic processes and systems, as well as aeronautics/aerodesign with the participation in this international collaborative effort.